2009

Analysis of prokaryotic community shift in anoxic estuarine sediment

William Berkeley Kauffman
San Jose State University

ANALYSIS OF PROKARYOTIC COMMUNITY SHIFT IN ANOXIC ESTUARINE SEDIMENT

A Thesis

Presented to

The Faculty of The Moss Landing Marine Laboratories

San José State University

In Partial Fulfillment

of the Requirements for the Degree

Master of Marine Sciences

by

William Berkeley Kauffman

August 2009

SAN JOSÉ STATE UNIVERSITY

The Undersigned Thesis Committee Approves the Thesis Titled

ANALYSIS OF PROKARYOTIC COMMUNITY SHIFT IN ANOXIC ESTUARINE SEDIMENT

by
William Berkeley Kauffman

APPROVED FOR THE MOSS LANDING MARINE LABORATORIES

Kenneth M. Coale 9/18/09
Dr. Kenneth Coale, The Moss Landing Marine Laboratories Date

Sabine Rech 9/18/09
Dr. Sabine Rech, San Jose State University Date

Ivano W. Aiello 9/18/09
Dr. Ivano Aiello, The Moss Landing Marine Laboratories Date

Dr. [signature] 9/15/09
Dr. Jeffery Hughey, Hartnell College Date

APPROVED FOR THE UNIVERSITY

[signature] 9/23/09
Associate Dean Office of Graduate Studies and Research Date

ABSTRACT

ANALYSIS OF PROKARYOTIC COMMUNITY SHIFT IN ANOXIC ESTUARINE SEDIMENT

by William Berkeley Kauffman

Prokaryotes mediate reduction-oxidation reactions resulting in the biological fluxes of hydrogen, carbon, nitrogen, oxygen, and sulfur, cumulatively representing five of the six major elements that serve as building blocks for biological macromolecules. In estuarine systems, prokaryotes are responsible for driving biogeochemical cycles and aid in the breakdown of pollutants in both the water column and the sediment. Understanding the microbial ecology of estuarine systems will elucidate the microbes' role in chemical cycling and estuarine health. In this study, denaturing gradient gel electrophoresis (DGGE) analysis of the 16S rRNA gene indicates a distinct shift in the sedimentary bacterial community at approximately 1 meter below the sediment-water interface at the head of Elkhorn Slough, the second largest estuary in California.

ACKNOWLEDGEMENTS

I would like to thank the following people and organizations for their help making this project work. Without the support of my family and friends, this project would have never gotten off the ground. I would first like to thank my mother Deborah Coffin and my sister Rebecca Kauffman. I am also indebted to committee members Kenneth Coale, Sabine Rech, Ivano Aiello, and Jeff Hughey. Your support and guidance has been invaluable. My friends and colleagues Jon Walsh, Max Overstrom-Coleman, Elaine Bryant, Sara Tanner, Craig Hunter, Jason Smith, Wes Heim, Allan Andrews, Adam Newman, Paula Mattheus, Cleber Ouverney, Liz Sassone, Cassandra Brooks, Brent Hughes, John Haskins, Paul Chua, Rhea Sanders, Brian Bender, Brian Dieter, and Mary Breton assisted with field and lab work and helped me maintain a degree of sanity throughout the process. Joan Parker and the MLML library staff all rock. JD, Scott and the small boats crew make fieldwork a breeze. James, Billy, Ralph and the rest of the facilities crew are always there to solve seemingly unsolvable problems, as are Jeff, Rhett and John in the IT department. Thank you all so much!

TABLE OF CONTENTS

LIST OF TABLES

LIST OF FIGURES

Introduction

Prokaryotes, the smallest of the Earth's living organisms, mediate reduction-oxidation reactions resulting in the biological fluxes of hydrogen, carbon, nitrogen, oxygen, and sulfur, representing five of the six major elements that serve as building blocks for all biological macromolecules (Falkowski, Fenchel, and Delong, 2008). The current oxidative state of our planet's surface results from the equilibrium between ancient photosynthetic microbial metabolism and tectonic and geothermal processes during the Archaean and Proterozoic eras combined with increased atmospheric oxygen levels due to the Paleozoic terrestrial plant explosion.

As in general ecology, a debate exists in the microbial ecology community concerning top-down versus bottom-up paradigms. Significantly, Lourens Baas-Becking's famous bottom-up hypothesis is often mistranslated from the original Dutch, "*alles is overall: maar het milieu selecteert*" (Baas-Becking, 1934). Literally, "Everything is everywhere: *but* the environment selects (italics mine)[i]" suggests that while microbes are universally distributed, local environmental conditions determine which species dominate and which are present in numbers below the detection limit (de Wit and Bouvier, 2006). In support of Baas-Becking's hypothesis, a review article published in Science concludes that prokaryotes are unlikely to be constrained by

---

[i] Lourens Baas-Becking's quote is often translated as "Everything is everywhere: and the environment selects" or "Everything is everywhere and the environment selects". The specific coordinating conjunction "but" is necessary to preserve the statement's intent because it recognizes the contradiction between observations specific microbes are observed in their characteristic environments and the idea that all microbes are cosmopolitan de Wit, R., and Bouvier, T. (2006) 'Everything is everywhere, but, the environment selects'; what did Baas Becking and Beijerinck really say? *Environmental Microbiology* **8**: 755-758.

geographical barriers (Finley, 2002). Rapid recombination rates, large species richness, large population numbers, short generation times, high dispersal rates, low speciation rates, and flat species-area curves associated with microbial populations suggest that microbial diversity will always be sufficiently high to respond to ecosystem changes (Finley, 2002). These traits contrast directly with biogeographical constraints that drive evolution in macroscopic organisms. Whereas macroorganisms primarily adapt their morphology in response to environmental change, microorganisms primarily adapt their metabolism.

The Baas-Beckian distribution model has come under attack recently (Green, Bohannan, and Whitaker, 2008). One study identified a biogeographic pattern in the distribution of the hyperthermophilic archaeon *Sulfolobus* at scales ranging from greater than 250 km to 6 km across the northern hemisphere (Whitaker, Grogan, and Taylor, 2003). A study of the global dispersal patterns of two other hot-spring microbes, *Synechococcus* and *Oscillatoria amphigranulata*, based on the highly conserved 16S ribosomal rRNA gene sequences, elucidated patterns of phylogeny and distribution consistent with geographical isolation (Papke, Ramsing, Bateson, and Ward, 2003). It is clear that certain biogeographical obstacles *are* capable of constraining certain microbes despite their dispersal abilities. Additionally, it is important to consider top-down selective pressures such as mortality inflicted by grazers and lytic viruses as well as community shaping-interactions such as symbiosis and allelopathy (Strom, 2008).

Microbes present interesting taxonomic problems. According to 16S rRNA gene sequence data, bacteria and archaea are the most diverse kingdoms of life, yet that

diversity is functionally unexplored. Morphological characteristics are limited while homologous recombination combined with lateral gene transfer allows members of different "species" to exchange genetic information, thereby obfuscating microbial evolutionary lineages (Achtman and Wagner, 2008). In fact, while some environments such as hot springs may lead to coherent clustering of DNA sequences similar to that in eukaryotic organisms, in other environments genetic diversity may be high enough to support a genetic continuum (Konstantinidis, Ramette, and Tiedje, 2006). The long-held view that microbes are exempt from dispersal limitations might simply be due to poor analytical resolution. Microbes with greater than 97% similarity across their ribosomal DNA are routinely assigned to the same species. "If that were done with animals," states Dr. Jessica Green of the University of California at Berkeley, "all primates from humans to lemurs would likely be lumped into one category, creating a group with far more cosmopolitan distribution and habits than any of the species erected by traditional naturalists" (Whitfield, 2005). She recommends adopting trait-based biogeography with a focus on micro- and macro-organismal interactions, thereby synthesizing biogeochemistry and microbial ecology and generating a novel science relevant to all domains of life (Green et al., 2008).

This study represents just such an attempt: to reconcile an observed sedimentary bacterial community shift with geochemical, physical, and biological data. This is a first look inside the black box that represents our understanding of the sedimentary microbial communities responsible for geochemical cycles in California's Elkhorn Slough. Researchers from the ocean drilling programs the Deep Sea Drilling Project (DSDP),

Ocean Drilling Project (ODP), and the International Drilling Project (IODP) found evidence of living microbial consortia in deep marine sediments to several hundreds of meters. Much is unknown about these communities, and while they are relatively inaccessible, estuarine sediments provide an accessible analogue to the "deep-biosphere" (Wilms, Kopke, and Sass, 2006a; Engelen & Cypionka, 2009). This study informs recent observations and discoveries with regard to the deep biosphere (D'Hondt, Jorgensen, and Miller, 2004; Schippers, Neretin, and Kallmeyer, 2005; Aiello and Bekins, 2008).

Elkhorn Slough is the second largest estuary in California. Elkhorn Valley was cut off from its headwaters by right-lateral movement along the San Andreas Fault during the mid-late Pleistocene. During the Last Glacial Maximum, approximately 20,000 years ago, sea levels were much lower, and present day Elkhorn Slough was a river valley. Gradually, as sea levels rose, a series of salt marshes developed along the landward margins of the coastal range that eventually migrated towards the present day center of Elkhorn Slough (Schwartz, Mullins, and Belknap, 1986). This study focuses on sediment deposited in the last 1,250 years.

In an estuary, sedimentary microbes exist in a state of dynamic equilibrium interrupted by episodic events such as flooding, resulting in rapid deposition and burial of benthic communities or temporarily increased rates of erosion. Nutrients are introduced from the water column by diffusive processes, and bioturbation, and ground water flow can be a significant source of microbial metabolites (Caffrey, Harrington, and Ward, 2002). Waste products from microbial activity are a source of electron acceptors for other microbes, resulting in biogeochemical profiles that, when viewed alone, can be

difficult to interpret in terms of microbial activity. While there have been both anthropogenic and natural changes affecting the Hudson's Landing study site, the biogeochemical processes involved are generalizeable to other systems.

In this study, molecular data from four depths ranging from 2.6 to 126 cm below the sea floor (cmbsf) were compared with the sediment's oxidation-reduction potential (ORP), carbon-nitrogen (C:N) ratio, chromophoric dissolved organic matter (CDOM), pH, magnetic susceptibility, mean grain size, and specific surface area. Modal analysis of the sediment size distribution data as well as core observations made during sampling and sub-sampling link these bacterial communities to other biological domains. A distinct shift in the bacterial consortia, from a *Proteobacteria* dominated denitrifying surface community to a more specialized fermentative community with fewer *Proteobacteria*, was detected by DGGE analysis between 100 cmbsf and 126 cmbsf. Coincident with this community shift was an increase in the diatomaceous sedimentary fraction, a decrease in C:N, a decrease in the magnetic susceptibility of the sediment, and increasing CDOM concentrations. The ORP did not change over this break. These observations represent a first look at the prokaryotic community composition of the sediment at Hudson's Landing in Elkhorn Slough.

Methods

Sample Collection

A 13.5 cm diameter core to a depth of 1.26 meters was taken from Hudson's Landing, a depositional site in Elkhorn Slough, with a pneumatic vibrating corer. To overcome the suction generated by removing a core from fine-grained sediments, an air tube was run alongside the outside of the core-tube and connected to the air source facilitating extraction. Coordinates for the site were 36° 51'18.30" N, 121° 45'37.61" W. The sediment core was capped and immediately transported to the lab. In an effort to minimize microbial contamination of the inner core, the overlying water was left in place and the core's center was sub-sampled the same day.

After visual examination, the core was photographed through the liner and immediately sub-sampled. The sediment was vertically extruded to minimize disturbance. The core was sliced in 1cm intervals (96 samples divided by 126 cm core results in a corrected interval of 1.3 cm). Immediately after each slice, a sediment sample was taken from the center of the freshly exposed face for molecular analysis using sterile 5mL syringes with the tips sliced off (Wilms et al., 2006a). Half of the molecular sample was archived at -80°C for future analysis. Reduction-oxidation potential was measured using a Cole Parmer combination ORP/pH soil electrode (cat. # EW-59001-75). The electrode was vertically inserted into the freshly exposed surface of the sediment to minimize oxidation that begins immediately upon exposure to air.

Organic Analysis

The remaining sediment was packed into 50 mL centrifuge tubes and spun at

1,500 rpm for 20 min to extract pore-water for analysis of chromophoric dissolved organic matter (CDOM). Absorption readings were taken at 1nm intervals from 200 to 800 nm using a scanning spectrophotometer fitted with quartz micro-cuvettes that minimize the volume of pore water required for analysis. Pore water pH was measured using an Orion Model 420A pH meter when sufficient water for analysis was obtained.

Sediment samples were dried at 30°C and homogenized by shaking in Teflon vials with steel beads. Particulate organic carbon: nitrogen ratios and % organic carbon were determined using a Perkin-Elmer 2400 Elemental Analyzer using a cystein standard. After homogenization, roughly 5 mg of the sediment was added to the sample capsule and weighed. Care was taken to avoid cross-contamination of samples and standards and the samples were stored in a dehumidifier until processing. Samples were run following the manufacturers protocol.

Sediment Analysis

Sedimentary grain sizes were analyzed using a Beckman Coulter LS 1230 laser particle size analyzer. Sediments from each 1.3 cm slice were homogenized and sonicated for 30 s to reduce clumping. The particle size analyzer detects clasts ranging from 2 mm to 0.04 μm. The mean particle size, primary modes, and specific surface area were calculated for each sample using Beckman Coulter software (Beckman Coulter, 2003).

Magnetic susceptibility was determined for each sample using an ASC Scientific Bartington Meter Model MS2. Three readings (SI Units) were taken from each centimeter and two ambient measurements were taken to correct for drift in the local

magnetic field. The difference between the average sediment reading and average ambient reading was recorded.

Smear slides were made in 5 sample intervals. A small amount of sample was mixed with water and spread onto a standard glass slide. After drying, an optically inert U.V. resin was used to mount a coverslip. The slide was fixed under ultraviolet light for 5 minutes. The slides were analyzed using a petrographic microscope to estimate the ratio of biogenic: terrigeneous sediment and to identify modal and compositional shifts in particle size.

DNA Extraction

Genomic DNA was extracted from the sediment samples using the PowerSoil DNA Isolation Kits (MoBio, Carlsbad, CA). The extraction was visualized on a 1.5% TAE agarose gel (non-denaturing) alongside a 1.5kb ladder (Promega, Madison, WI).

Polymerase Chain Reaction for Bacteria. A 566 base pair section of the extracted 16S rDNA gene was amplified with the universal bacterial 16S rRNA gene sequence G-C clamped primer set GC341F (5'-CGCCCGGGGCGCGCCCCGGGCGG GGCGGGGGCACGGGGGGCCTACGGGA GGCAGCAG-3') and 907R (5'-CCGTC AATTCMTTTMGTTT-3') (Wilms et al., 2006b). All amplifications were run using GoTaq Colorless Master Mix (Promega, Madison, WI). All amplifications were run with an annealing temperature of 55°C and MgCl concentration of 1.5μM, primer concentration of 1μM and nucleotide concentration of 200μM. The PCR parameters were as follows: Initial denaturation of 95°C for 2 min followed by 34 cycles of 95°C for 30 sec, 55°C for 30 sec, and 72°C for 30 sec; and a final extension at 72°C for 7 min. The

product was electrophoresed on a 1.0% agarose gel alongside a 100bp ladder (Promega, Madison, WI), stained with a 1% solution of ethidium bromide, and visualized under U.V. light.

Archaea. Extracted DNA were amplified with the universal archaeal 16S rRNA gene sequence G-C clamped primer set GC357F (5'-CGCCCGCCGCGCGCGGCGGGC GGGGCGGGGGCACGGGGGGCCCTACGGGGCGCAGCAG-3') and 915R (5'-CTGC TCCCCCGCCAATTCCT-3'). All amplifications were run with a MgCl concentration of 1.5μM using a touchdown protocol where the annealing temperature was to be dropped by 0.5°C every cycle from a maximum of 65°C to a minimum of 55°C. The PCR program was as follows: Initial extension of 95°C for 2 min; 21 cycles of 94°C for 1 min; 65°C for 1 min; 72°C for 3 min with a 0.5°C decrease in annealing temp each cycle until 55°C is reached; followed by 10 cycles of 94°C for 1 min; 55°C for 1 min; 72°C for 3 min; and a final extension of 72°C for 30 min. The PCR product was electrophoresed on a 1.0% agarose gel alongside a 100bp ladder (Promega, Madison, WI), stained with a 1% solution of ethidium bromide, and visualized under U.V. light.

Denaturing Gradient Gel Electrophoresis

Denaturing Gradient Gel Electrophoresis analysis was carried out using the BioRad DCode system following the manufacturers protocol (Zwart and Bok, 2004). Biorad's Model 475 Gradient Former was used to cast 6% polyacrylamide gels (with 2% v/v glycerol added for increased flexibility) with a denaturant gradient between 35% and 60% urea: formamide (100% corresponds to 7M urea and 40% formamide by volume). The samples were electrophoresed at 75V for 999 min. Gels were stained with ethidium

bromide, visualized, and photographed under ultraviolet light. Bands of interest were stabbed with a sterile pipette tip and added to 50μL sterile water at room temperature. Excised bands were incubated at 4°C for at least 24 hours to allow diffusion of DNA into the solution. 1μL of this solution was used as template for amplification to construct the clone library.

Polymerase Chain Reaction for Generation of Clone Library

Bacteria. DNA from band excisions were amplified with the universal bacterial 16S rRNA primer set 314F (5'-CCTACGGGAGGCAGCAG-3') and 907R (5'-CCGTCAATTCMTTTMGTTT-3'). All amplifications were run following the protocol described previously and electrophoresed on a 1.0% agarose gel alongside a 100bp ladder, stained with ethidium bromide, and visualized under U.V. light.

Archaea. Extracted DNA was amplified with the universal archaeal 16S rDNA primer set 357F (5'-CCCTACGGGGCGCAGCAG-3') and 915R (5'-CTGCTCCCCCGCCAATTCCT-3'). All amplifications were run following the protocol described previously and electrophoresed on a 1.0% agarose gel alongside a 100bp ladder, stained with ethidium bromide, and visualized under U.V. light.

Clone Library Construction

The amplified products were purified with a PCR clean-up Kit (Bay Gene Inc., San Francisco, CA). In preparation for the construction of a clone library, bacterial and archaeal PCR products were ligated to a 1.5kb plasmid vector using T4 DNA ligase in ATP buffer with the pGEM-T Easy Vector System I (Promega, Madison, WI). Purified PCR product was added to achieve a product: vector ratio of 3:1.

The ligated PCR product was transformed into competent *E. coli* cells. The cells containing the plasmid DNA were selected for by incubation in super optimal broth with catabolite repression (SOC) with ampicillin (100μg/mL). The transformed cells were incubated at 37°C for 1.5 hrs and plated on duplicate Luria-Bertani agar (LB) plates fortified with ampicillin (100μg/mL), isopropyl thiogalactoside (IPTG) (0.5mM), and 5-bromo-4-chloro-3-indolyl-beta-D-galactopyranoside (X-Gal) (80μg/mL). The plates were incubated for 18 hrs at 37°C to allow for the formation of bacterial colonies.

Successfully transformed cells acquire the plasmid that contains an ampicillin resistant gene. Only cells that have accepted the plasmid are able to grow on the LB plates. Blue-white screening was used to select only successfully transformed bacterial colonies containing the 16S rDNA gene insert for further analysis.

Two white colonies from each plate (4 samples per excised DGGE band labeled A, B, C, D) were randomly selected to inoculate tubes containing 5mL of LB broth with ampicillin (100μg/mL). The tubes were incubated on a heated shaking table at 37°C for 24 hrs at 150 rpm. A plasmid prep kit (Bay Gene, San Francisco, CA) was used to extract the plasmid from the resulting bacterial colonies. Five μl of the DNA solution was digested using EcoR1 restriction endonuclease, electrophoresed on 1% TAE/agarose gels, stained with ethidium bromide, and visualized under U.V. light to verify the presence of the DNA amplicon of interest. The concentration of DNA in the plasmid prep product was quantified using the NanoDrop spectrophotometer.

Samples are named by the depth where they were collected with the DGGE band number and transformed colony letter appended. Sample 2cm-1A was collected from 2

cmbsf, extracted from the DGGE band nearest the well (lowest GC content), and represents the first colony selected following blue-white screening.

Sequencing and Phylogenetic Analysis

Sequencing was performed by Sequetech (Mountain View, CA) using the Applied Biosystems 3730xl DNA Analyzer. Phylogenetic analysis was conducted on a Macintosh Powerbook G4 running OSX 10.4.11, with the exception of the multiple sequence alignment.

Raw sequences were analyzed using 4PEAKS. The sequences were screened for vectors using the BLAST Vector Screen command. In some cases the quality of the 5' end of the sequence was poor and sequences were trimmed to approximately 500 bp.

A global 16S rRNA gene multiple sequence alignment was created using NAST on the greengenes.lbl.gov server. Each sequence was compared to over 9000 Operational Taxonomic Units (OTU's) previously identified solely by sequence identity clustering. Simultaneously, Simrank (an N-mer comparison tool) was used to find the nearest non-chimeric neighbors from the entire greengenes database (NCBI and RDP) for use as a backbone for the phylogeny.

To identify duplicate samples, a distance matrix was constructed using PAUP 4.0 (Swofford, 2002). Samples with <1% mean character difference were considered duplicates and only one was used in for the construction of the phylogenetic tree. Select nearest neighbor isolates were included in the matrices to quantify relatedness.

Phylogenetic trees were constructed using PAUP 4.0 (Swofford, 2002). Likelihood ratio test statistics (-lnL) for 56 substitution models were calculated as twice

the difference between the log likelihood scores of the two models contrasted. When the model representing the null hypothesis is a special case of the alternate model, this statistic fits a chi-square distribution where the degrees of freedom are equal to the number of freely varying parameters between the two models. The appropriate substitution model for both the archaeal and bacterial trees was determined using the AIC model selection criterium on ModelTest Server 1.0 using branch lengths as parameters and a confidence level of 0.01 (Posada, 2006). For the bacterial tree, model TrN+I+G was selected (-lnL= 40891.3828; K=206). The base frequencies for the model are as follows: freqA=0.2416; freqC=0.2229; freqG=0.2938; freqT=0.2417. The Rate Matrix for this model was: R(a) [A-C]=1.0000; R(b) [A-G]= 2.3190; R(c) [A-T] = 1.0000; R(d) [C-G] = 1.0000; R(e) [C-T] = 3.4678; R(f) [G-T] = 1.0000. The proportion of invariable sites was 0.1927 and the gamma distribution shape parameter was 0.6429.

For the archaeal tree, model TrN+I+G was also selected (-lnL= 9390.3398; K=36). The base frequencies for the model were as follows: freqA=0.2320; freqC=0.2321; freqG=0.3210; freqT=0.2149. The Rate Matrix for this model was: R(a) [A-C]=1.0000; R(b) [A-G]= 2.3921; R(c) [A-T] = 1.0000; R(d) [C-G] = 1.0000; R(e) [C-T] = 4.6944; R(f) [G-T] = 1.0000. The proportion of invariable sites was 0.2544 and the gamma distribution shape parameter was 1.0009.

For both the bacterial and archaeal trees, a full heuristic search was conducted in PAUP 4.0 on the aligned sequences using the maximum likelihood criterium defined by model TrN+I+G. The starting trees were obtained using stepwise addition. The addition sequence as-is was used, holding one tree at each step of the addition process. The Tree-

Bisection-Reconnection (TBR) branch swapping algorithm was selected and branches were collapsed if their length was less than or equal to 1e-08.

The Crenarchaeaote *Caldisphaera dracosis str.* 18U65 was selected as the outgroup for the bacterial phyla and the Gammaproteobacterium *Stenotrophomonas maltophilia* str. E2 was designated as the outgroup for the archaeal tree. The bacterial tree was subjected to maximum parsimony bootstrap analysis (n=10,000) using the accelerated transformation method for optimizing characters (Felsenstein, 1985). Gaps were treated as missing data. The archaeal tree was subjected to maximum likelihood bootstrap analysis (n=1,000) using the parameters described previously. The trees were edited using FigTree v1.2 and Adobe Photoshop CS.

Partial 16S rRNA gene sequences were submitted to GenBank and are filed under accession numbers FJ609949 - FJ609979.

Results

The core was taken on a rising tide from 36° 51'18.30"N, 121° 45'37.61"W on 9/10/2007 from Hudson's Landing in Elkhorn Slough (Figure 1). A long-term monitoring study reported that the overlying water temperature was 20.64°C, with a salinity of 33.36‰. Dissolved oxygen was at 88.4% saturation or 200.6 μM/L, the pH was 7.94, the ammonium concentration was 6.67 μM/L, and orthophosphate concentrations were 4.38 μM/L. These data were collected on September 11, 2007 (Hughes and Haskins, 2007) and fall within previously reported ranges (Caffrey et al., 2002; Caffrey, Harrington, Solem, and Ward, 2003).

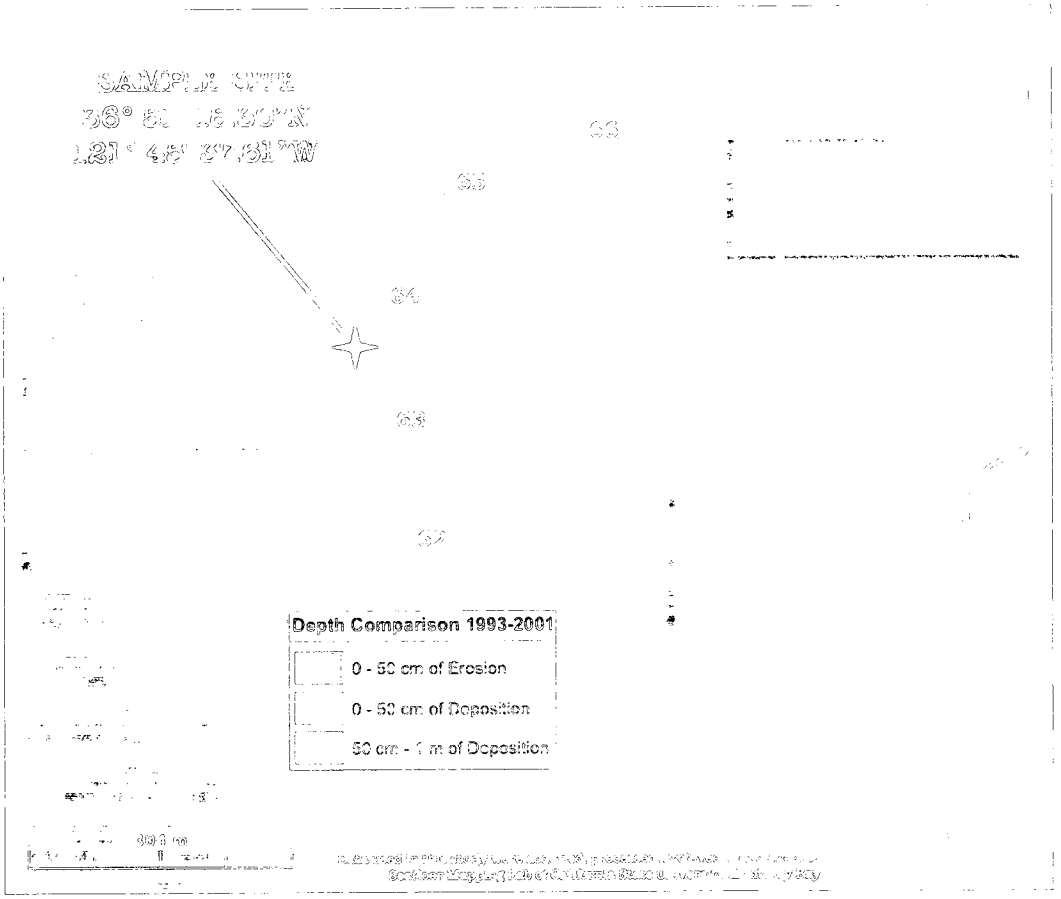

Figure 1. Hudson's Landing, Elkhorn Slough. CSUMB seafloor mapping data show that the area was a depositional environment between 1993-2001.

The sediment core was retrieved with an undisturbed sediment-water interface (Figure 2). The benthic layer was covered with unidentified tubeworm burrows. Amphipods and copepods were observed in the overlying surface water. The worm burrows were observed to a depth of approximately 15 cmbsf and in the absence of any other burrowing macrofauna this may be considered a bioturbation zone. Fecal pellets dominated the flocculent, uppermost sediments and when disturbed the smell of the released bubbles indicated they contain hydrogen sulfide and possibly methane although

captured gases were not flammable. Similar sediments exposed during low tides exhibited a distinct layer of jet-black material (likely reduced iron species) immediately below an oxidized crust.

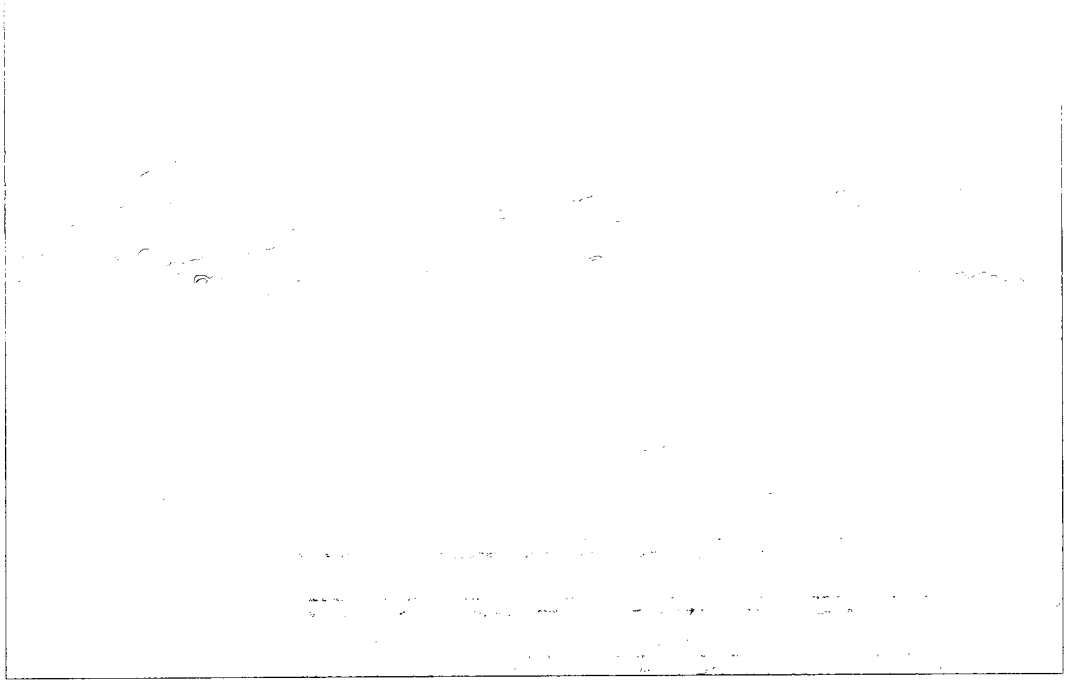

Figure 2. Surficial Sediment. View of the top of the sediment core immediately before sub-sampling. The undisturbed surface is covered with tube-worms. These worms burrow into the sediment (as can be seen in the lower left corner of the picture) and pump in overlying water thereby disturbing the geochemical gradients and generating a zone of bioturbation. The worm burrows were present to approximately 15 cm, the depth at which ORP and pH readings stabilize.

Oxidation-Reduction Potential (ORP)

The ORP ranged from approximately -150mV to -175mV (Figure 3). The ORP decreased slightly in the upper 40 cm; however below the zone of bio-irrigation the values are stable.

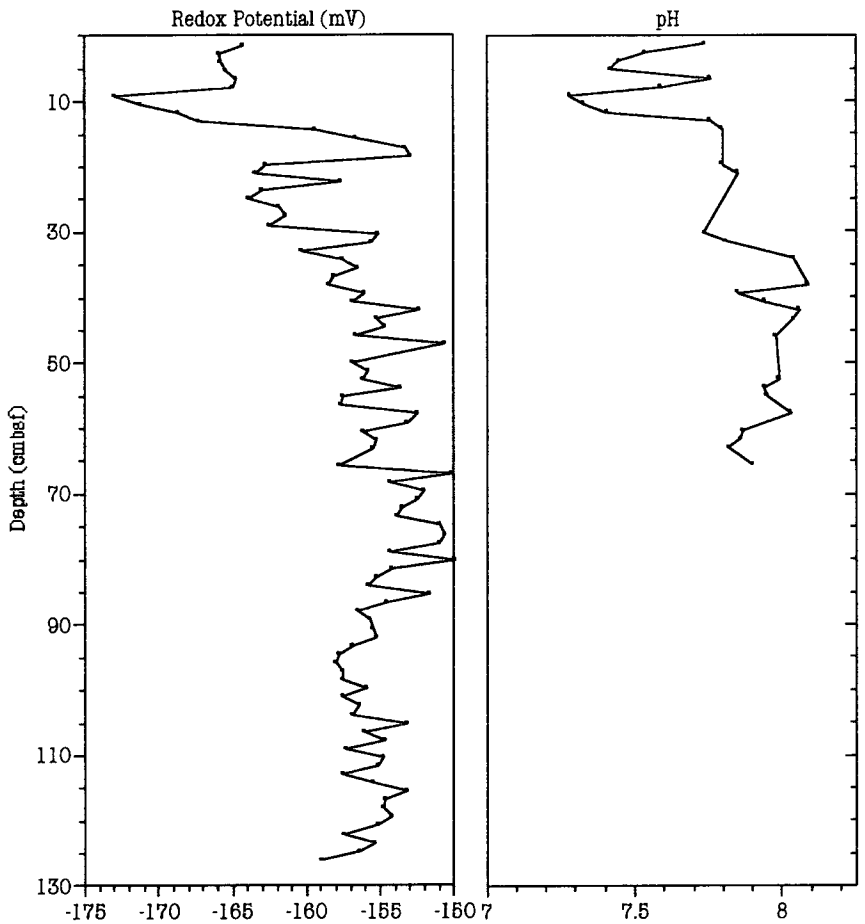

Figure 3. Oxidation-Reduction Potential and pH. Vertical insertion oxidation-reduction measurements range approximately -150 mV to -175 mV. With a margin of error of 25 mV, these values are considered to be unchanging throughout the core and thermodynamically favor sulfate reduction and methanogenesis. pH measurements were taken from the pore water post-centrifugation when sufficient pore water could be extracted. The decrease with depth likely results from the bacterial degradation of organic acids.

Pore water pH was recorded to a depth of approximately 70 cmbsf after centrifugation. Beyond 70 cmbsf, the volume of extracted pore water had diminished such that accurate and precise measurements could no longer be obtained. The pH in the upper 70 cmbsf was positively correlated with the ORP and gradually increases from pH=7 to pH=8. Gradually increasing pH with depth was likely due to increasing microbial degradation of organic acids (Hambrick III, DeLaune, and Patrick, 1980) and proton scavenging activity of fermentative bacteria in the deeper sediment.

Carbon: Nitrogen Analysis

Chromophoric Dissolved Organic Material (CDOM) values increased with depth (Figure 4). Particulate organic carbon (POC) and particulate organic nitrogen (PON) values are somewhat variable to 100 cmbsf and increased to 126 cmbsf. Carbon: nitrogen ratios are positively correlated with POC and PON until 100 cmbsf where the carbon: nitrogen (C: N) ratio decreases with increasing POC and PON values.

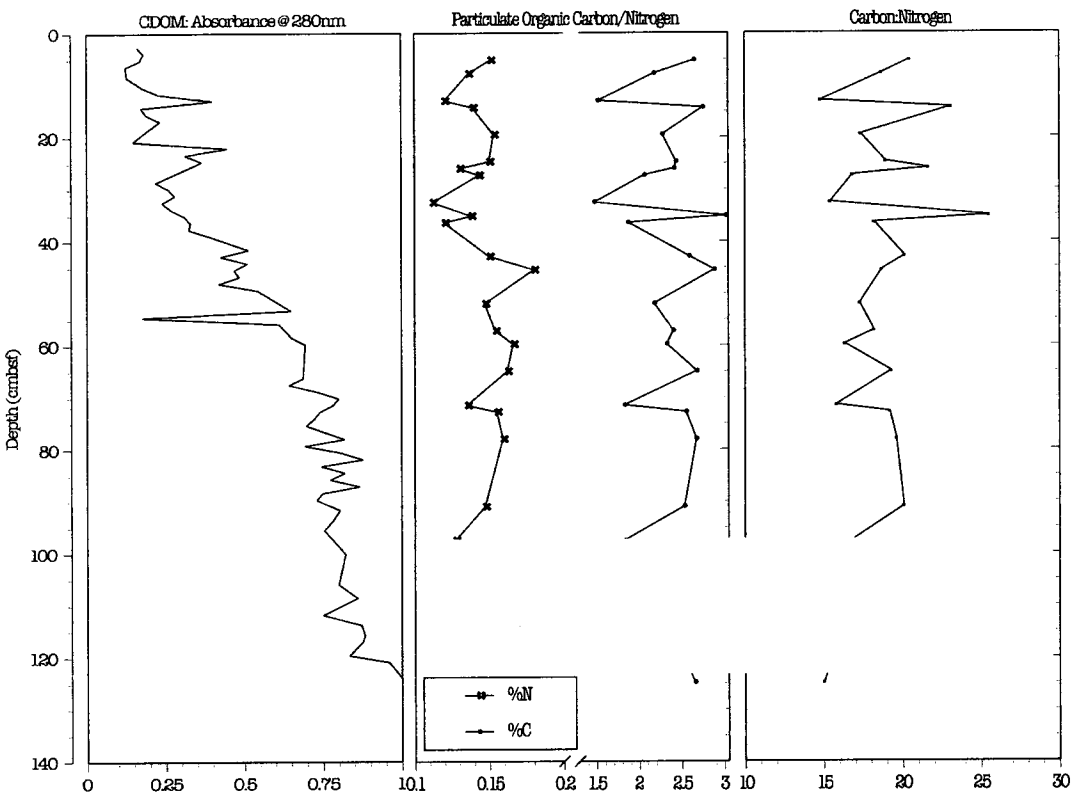

Figure 4. Carbon/ Nitrogen Data. Chromophoric dissolved organic carbon (CDOM), % organic carbon, % organic nitrogen, and atomic C:N ratios are plotted here against sediment depth (cm). CDOM values decrease with depth as a result of the accumulation of humic acids and other recalcitrant organic material in the pore water. POC and PON values vary downcore representing changing depositional environments. The C:N data follows the POC and PON data until 100cm (highlighted) when the ratio decreases. This is likely evidence of selective degradation of organic matter components and/or a change in the carbon source from primarily cellulosic vascular plant material (C:N ratios of 20 and above) to a depositional regime with a greater fraction of carbon derived from algae and planktonic sources (C:N ratios of 10 and 6 respectively).

Lithologic Data

Together, the physical data record a shift in the depositional environment at roughly 100 cmbsf (Figure 5). Magnetic susceptibility readings varied slightly down-core, however they decreased significantly below 100 cmbsf indicating the presence of a smaller ferromagnetic fraction in the sedimentary matrix, likely due to a reduction in the terrigeneous component in the sediment. There were small fluctuations in the mean particle size of the sediment, however all values fell in a relatively small range (5-12 μM). Specific surface area (m^{-1}) is a derived value used to determine the type and properties of sediment obtained by dividing the surface area by the volume. Diatomaceous tests have higher specific surface areas than mineral clasts of equal diameter. Despite a consistent particle mean, specific surface area measurements increase sharply at 100 cmbsf.

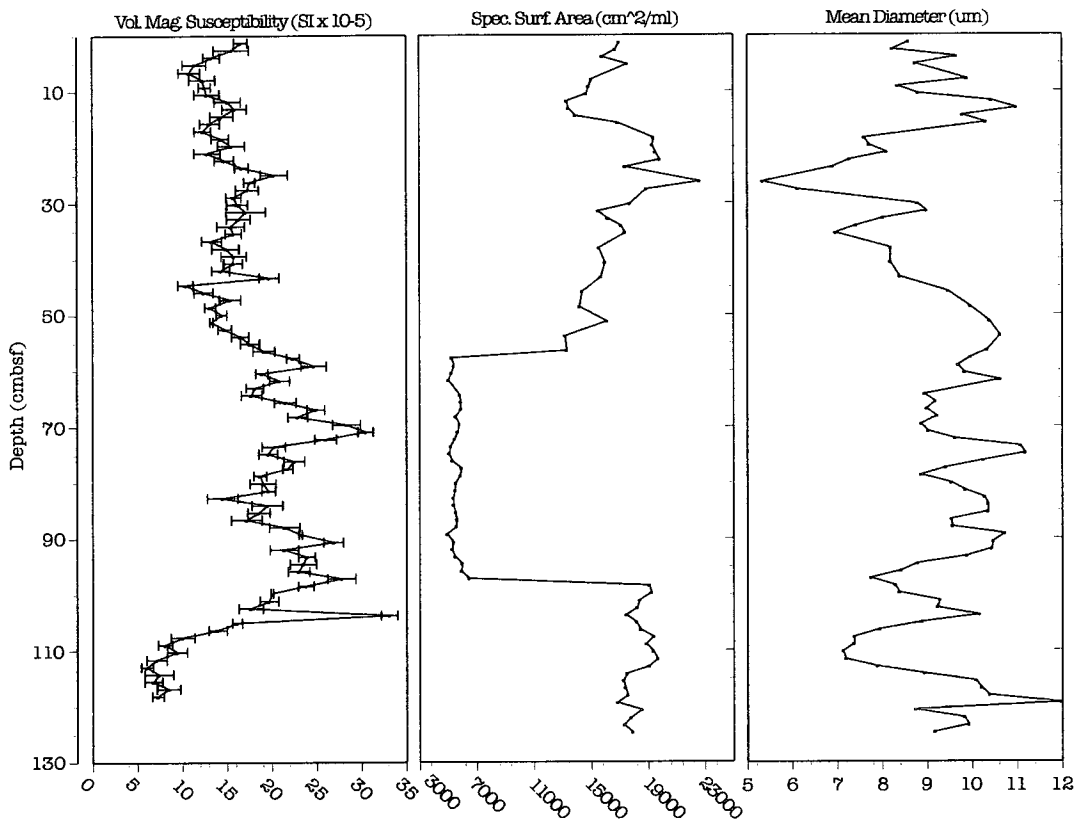

Figure 5. Lithologic Data. Magnetic susceptibility readings range from approximately 5 to 30 SI units. The large magnetic reading taken at 105 cm may be an outlier. Variations likely reflect a changing depositional environment, as higher values are associated with increased fluvial deposits while lower values indicate a larger biological sedimentary fraction. The sharp drop at roughly 100 cm is coincident with a doubling of the specific surface area. The increase in surface area beyond 100 cm is attributed to an increase in diatom frustules. A similar trend is not noticeable in the mean particle size data suggesting an energetically stable depositional environment.

Smear Slides

Smear slides made from sediment samples above and below the observed shift in bacterial community structure at 100 cmbsf suggest that the change in magnetic susceptibility, the change in the C:N values, and the change in specific surface area measurements were due to the abundance of diatoms in the 100-126 cmbsf portion of the sediment core (Figure 6,7, 8, 9). Frequency plots describing the results of the grain size analyses show three modes per sample that do not change significantly throughout the core (Figure). The observed modes are described in tabular form (11). The dominant mode ranged from 10-14 μm, the secondary mode ranged from 37-50 μm, and the tertiary mode ranged from 128-154 μm. Although the modes remained constant, the data illustrate that the modal composition shifted from mineral dominated deposits to diatom-dominated deposits below 100 cmbsf.

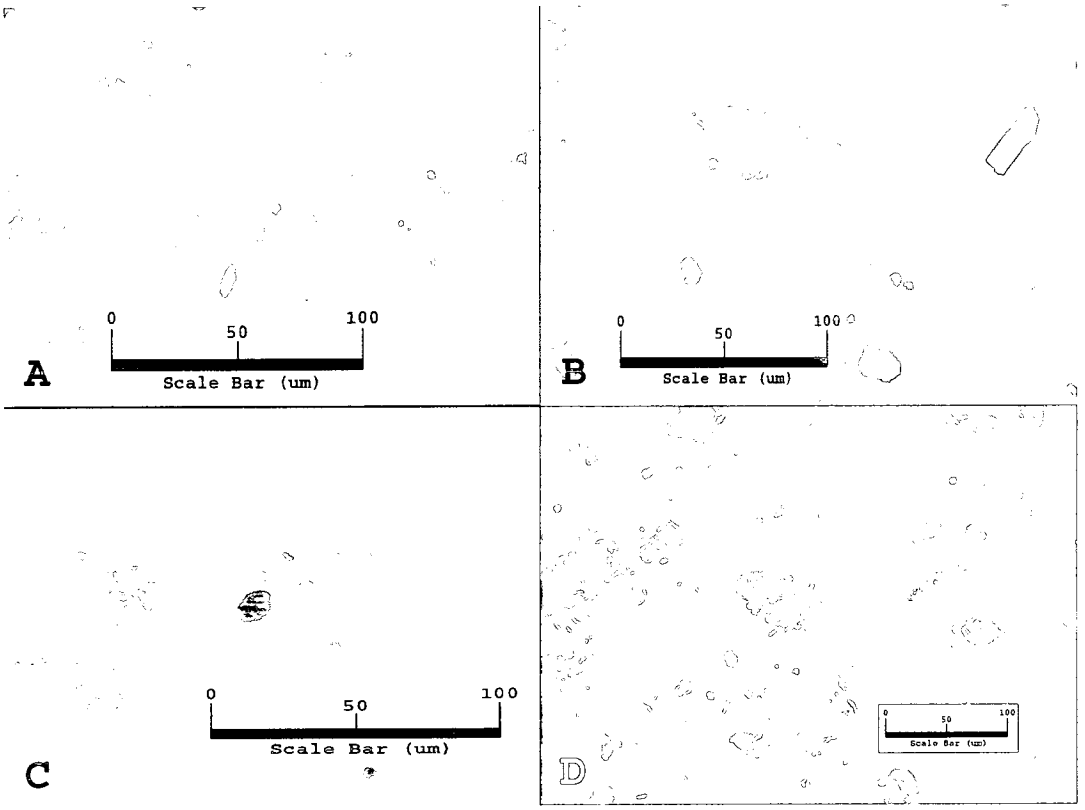

Figure 6. Sediment Photos at 2.6 cm. Images representative of the three modes detected at 2.6 cm. The primary mode (2.647% @ 11.29 μm) consists primarily of silt. The secondary mode (1.4% @ 40 μm) is a mix of diatom fragments, clay minerals, and organic detritus. The tertiary mode (1.210% @ 153.8 μm) (A) is composed of organic material likely of terrestrial origin. Note that although diatom fragments are present (C) they are of the same diameter as the equally abundant mineral fragments (B center) and smaller bits of plant matter (B center-right). Photo D is an image taken under cross-polorization showing the dominance of quartz and feldspar.

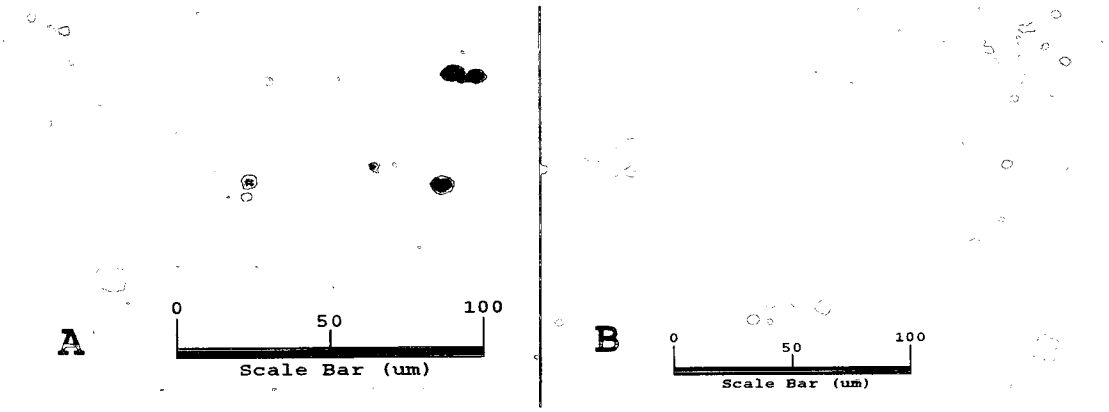

Figure 7. Sediment Photos 53 cm. Images representative of the three modes detected at 53 cm. The primary mode (2.911% @ 12.40 μm) consists primarily of clay minerals. The secondary mode (1.669% @ 37.97 μm) contains a few diatom fragments, but is mostly quartz, feldspar, and organic detritus. The tertiary mode (1.093% @ 140 μm) (B) is composed of clumped organic material.

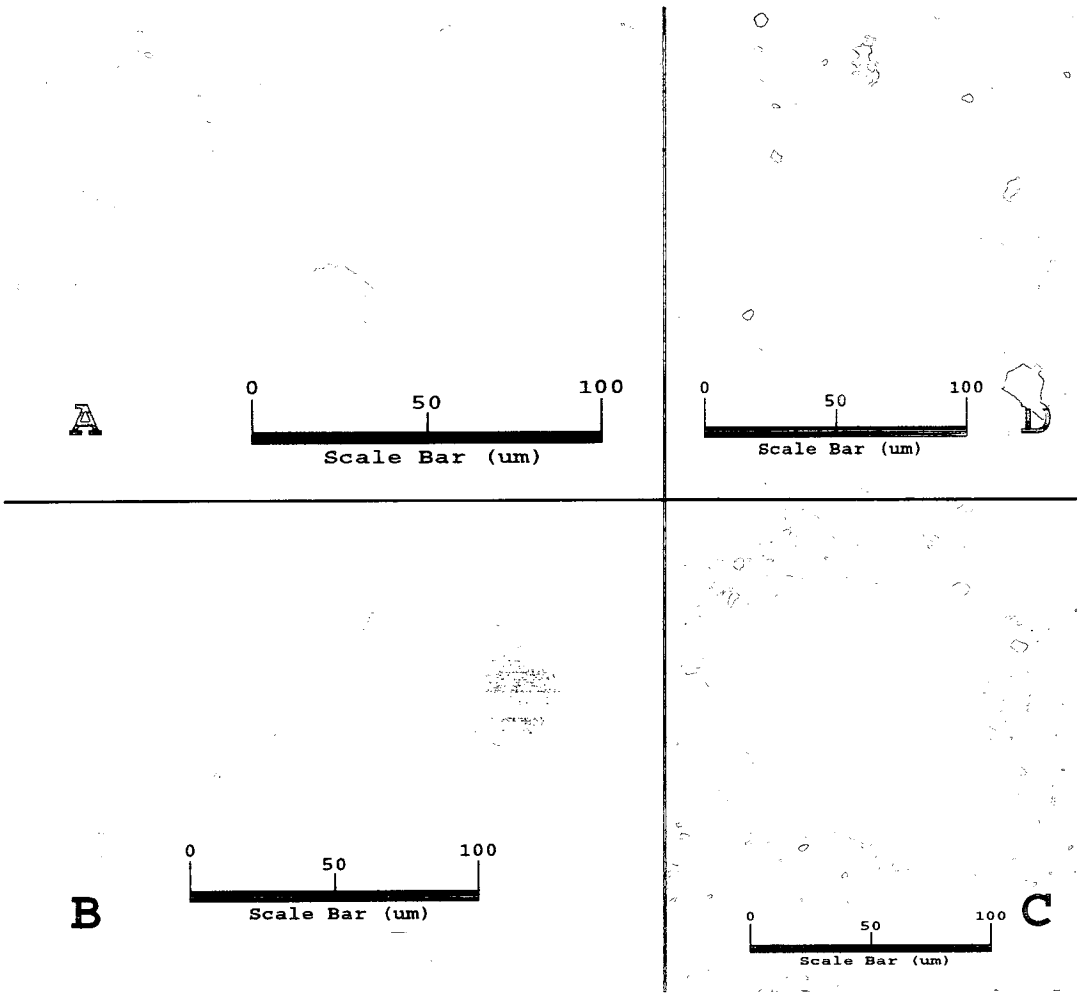

Figure 8. Sediment Photos 93 cm. Images representative of the three modes detected at 93 cm. The primary mode (2.908% @ 12.4 μm) consists primarily of silt. The secondary mode (1.635% @ 50.22 μm) is a mix of diatoms (A, B) and aggregated smaller clasts bound by organic material (A). There are also quartz and feldspar particles in this size class. The tertiary mode (1.032% @ 168.9 μm) is composed primarily of larger fecal pellets (D).

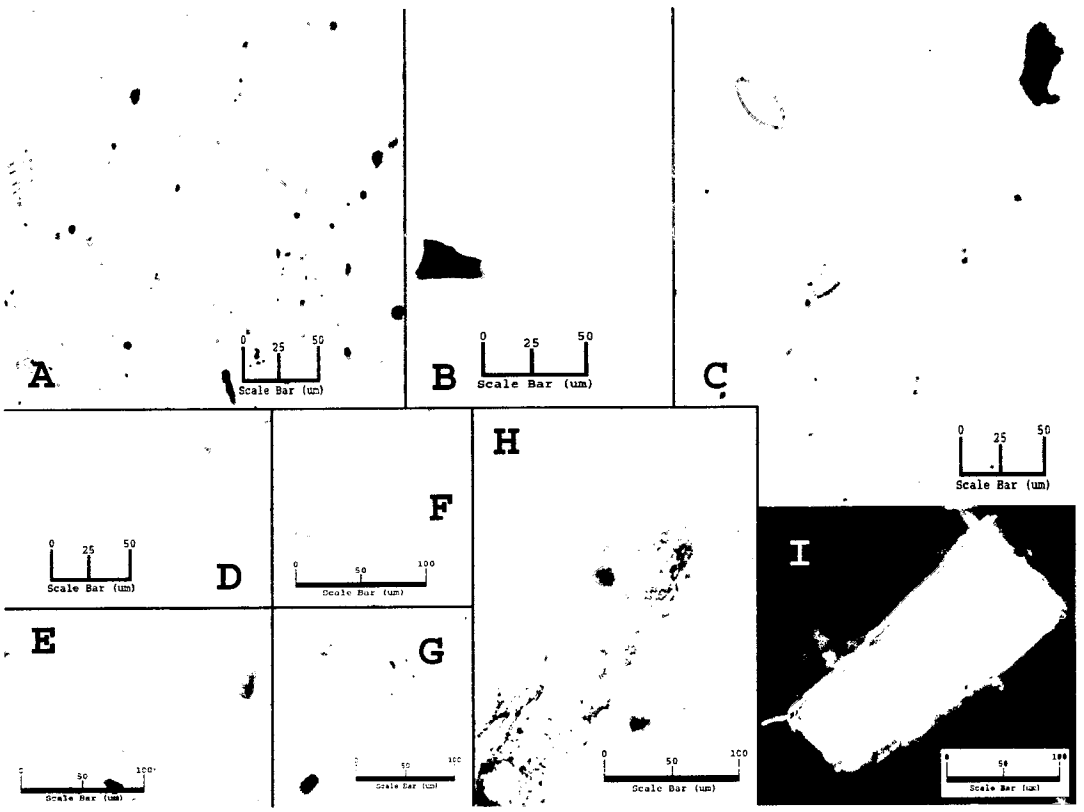

Figure 9. Sediment Photos 126 cm. Images representative of the three modes detected at 126 cm. The primary mode (2.695%% @ 13.61 μm) consists primarily of clay minerals. The secondary mode (1.560% @ 41.68 μm) is almost exclusively complete or partially fragmented diatoms (A, C), with occasional fragments of quartz, feldspar, and organic detritus (A, B, C). The tertiary mode (1.177% @ 153.8 μm) is composed of large pennate diatoms (A, B, D, E, F, G) some well preserved organic material (H) and unidentified well textured calcite (I).

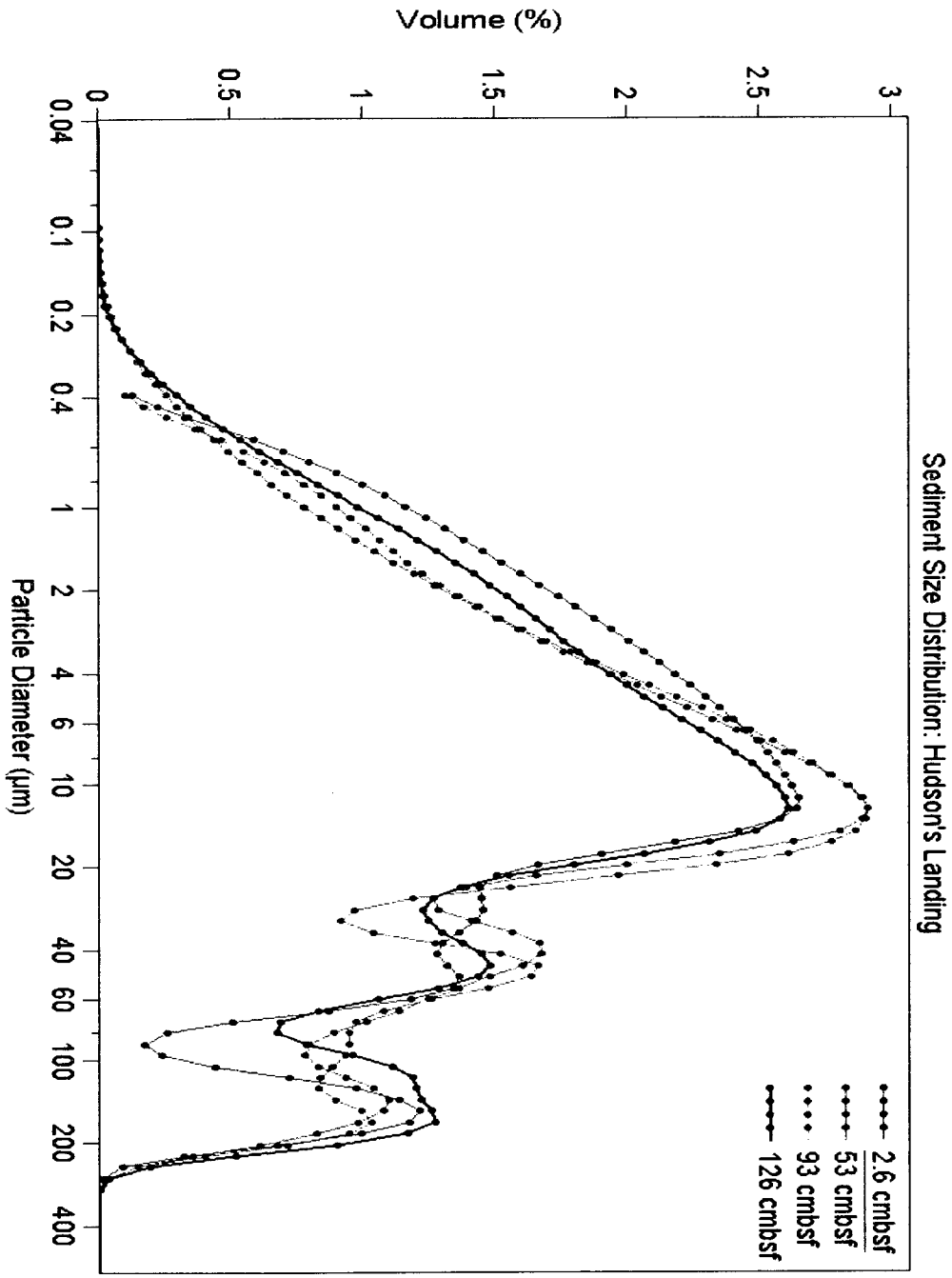

Figure 10. Particle Size Distributions at 2.6 cm, 53 cm, 93 cm, and 126 cm. Particle size means and modes do not change significantly with depth.

Table 1

Sediment Modal Data

Depth	Primary Mode	Secondary Mode	Tertiary Mode
2.6 cm	11.29	39.46	153.8
53 cm	12.4	37.97	140.0
93 cm	12.4	50.22	168.9
126 cm	13.61	41.68	153.8

. Particle size analysis indicates three modes per sample that do not change significantly throughout the core. The dominant mode ranged from 10-14 μm, the secondary mode ranged from 37-50 μm, and the tertiary mode ranged from 128-154 μm.

Molecular Data

Denaturing gradient gel electrophoresis. Although DGGE data indicated a shift in the bacterial consortia between 100 and 126 cmbsf (Figure 6) the data did not indicate a shift in the archaeal consortia over the depths sampled. Only three bands were identifiable in the DGGE lanes for all archaeal samples. Because of limited sampling, the remaining archaeal GC-clamped PCR products were studied from all depths in a single DGGE lane (hereafter referred to as AMIX). In this case, the dominant bands were sampled under the assumption that equivalent bands from adjacent samples represent the same taxonomic unit.

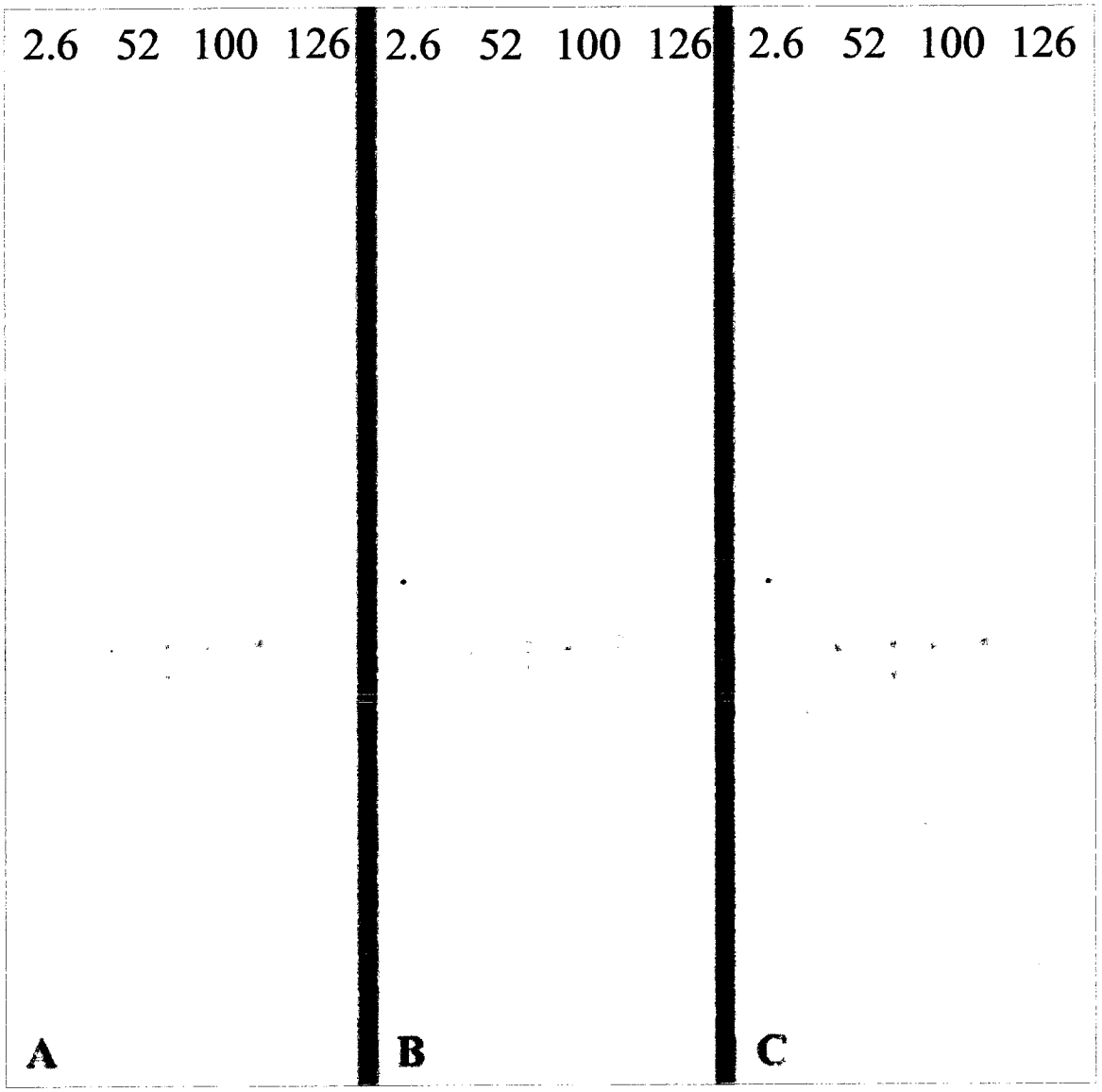

Figure 11. Denaturing Gradient Gel Electrophoresis (DGGE) Gel Photo. (A). Raw image of DGGE gel. These samples were run through a 6% acrylamide gel with 2% glycerol (v/v) added for increased flexibility. The urea gradient of 35%-60% is topped with a 0% stacking gel. The samples were electrophoresed for 999 min at 75 volts. (B). Identical DGGE image with all major bands highlighted. Adjacent bands are assumed to represent identical bacterial taxa. Note the difference in banding patterns between 100 cmbsf and 126 cmbsf (C). Identical DGGE image with bands highlighted that were selected for cloning and sequencing.

Phylogenetic and similarity analyses. Of the 30 16S rRNA gene sequences obtained, ten were identified as *Euryarchaeota* and *Crenarchaeota*. None of the clones was identical to any of the known sequences in the NCBI or RDP databases. Two of the bacterial clones amplified with the primer set designed to target bacteria aligned with Archaea. Similarity analysis indicated that 6 of these clones (including the species showing specificity for the bacterial primer set) were duplicates (<1% different) leaving 4 unique archaeal sequences (Figure 7). Three of the four unique sequences were obtained from the uppermost DGGE band indicating that DNA from multiple species possess similar GC ratios and the resolution was not sufficient to distinguish between OTU's in some cases. One unique sequence was obtained from the second major DGGE band indicating the presence of only one archaeal species with a higher GC content.

Organism	*Methanobrevibacter gottschalkii str. PG*	*Methanobrevibacter sp str. RT*	*Thermofilum pendens str. Hvv3 DSM 2475*	*Staphylothermus achaiicus*	*Desulfurococcus mobilis*	*Cenarchaeum symbiosum*	*Caldisphaera lagunensis str. IC-154*	*Methanobrevibacter sp. str. FM1*	*Thermofilum pendens str. Hrk 5*	*Caldisphaera dracosis str. 18U65*	*Nitrosopumilus maritimus str. SCM1*	*Stenotrophomonas maltophilia str. E2*	AMIX 1D	AMIX 2C	AMIX 1A	AMIX 1B
Methanobrevibacter gottschalkii str. PG	X															
Methanobrevibacter sp str. RT	0.06	X														
Thermofilum pendens str. Hvv3 DSM 2475	0.25	0.25	X													
Staphylothermus achaiicus	0.24	0.25	0.11	X												
Desulfurococcus mobilis	0.25	0.25	0.13	0.04	X											
Cenarchaeum symbiosum	0.28	0.28	0.25	0.23	0.25	X										
Caldisphaera lagunensis str. IC-154	0.25	0.25	0.17	0.12	0.14	0.25	X									
Methanobrevibacter sp. str. FM1	0.07	0.07	0.24	0.22	0.24	0.29	0.24	X								
Thermofilum pendens str. Hrk 5	0.25	0.25	**0.00**	0.11	0.13	0.25	0.17	0.24	X							
Caldisphaera dracosis str. 18U65	0.25	0.25	0.17	0.12	0.14	0.26	0.03	0.24	0.17	X						
Nitrosopumilus maritimus str. SCM1	0.27	0.27	0.24	0.23	0.24	0.06	0.25	0.27	0.24	0.26	X					
Stenotrophomonas maltophilia str. E2	0.35	0.35	0.35	0.33	0.34	0.37	0.35	0.34	0.35	0.36	0.37	X				
AMIX 1D	0.27	0.27	0.19	0.20	0.20	0.26	0.22	0.26	0.19	0.22	0.26	0.40	X			
AMIX 2C	0.28	0.27	0.22	0.22	0.21	0.17	0.22	0.25	0.22	0.22	0.16	0.37	0.21	X		
AMIX 1A	0.20	0.20	0.26	0.26	0.27	0.31	0.26	0.20	0.26	0.26	0.30	0.36	0.30	0.29	X	
AMIX 1B	0.24	0.23	0.18	0.17	0.17	0.26	0.19	0.21	0.18	0.19	0.26	0.36	0.16	0.20	0.27	X
Mean Character Differences: Adjusted for Missing Data																

Figure 12. 16s rRNA Gene Sequence Similarity Matrix for Archaea.

Maximum-likelihood phylogenetic analysis of the 16S rRNA gene on eleven known archaeal taxa and the four samples from Hudson's Landing identified two clades (Figure). The *Euryarchaeota* was represented by the first clade and showed strong bootstrap support (Bootstrap Proportion Values (BP)=88). In this clade, three *Methanobrevibacter* grouped with AMIX-1A. Sister to this clade was an unsupported *Crenarchaeota* with one well supported (BP=97) and one poorly supported (BP=63) lineage. Slough samples AMIX-1B, AMIX-1D, and AMIX-2C all clustered with *Nitrosopumilus* and *Crenarchaeum*.

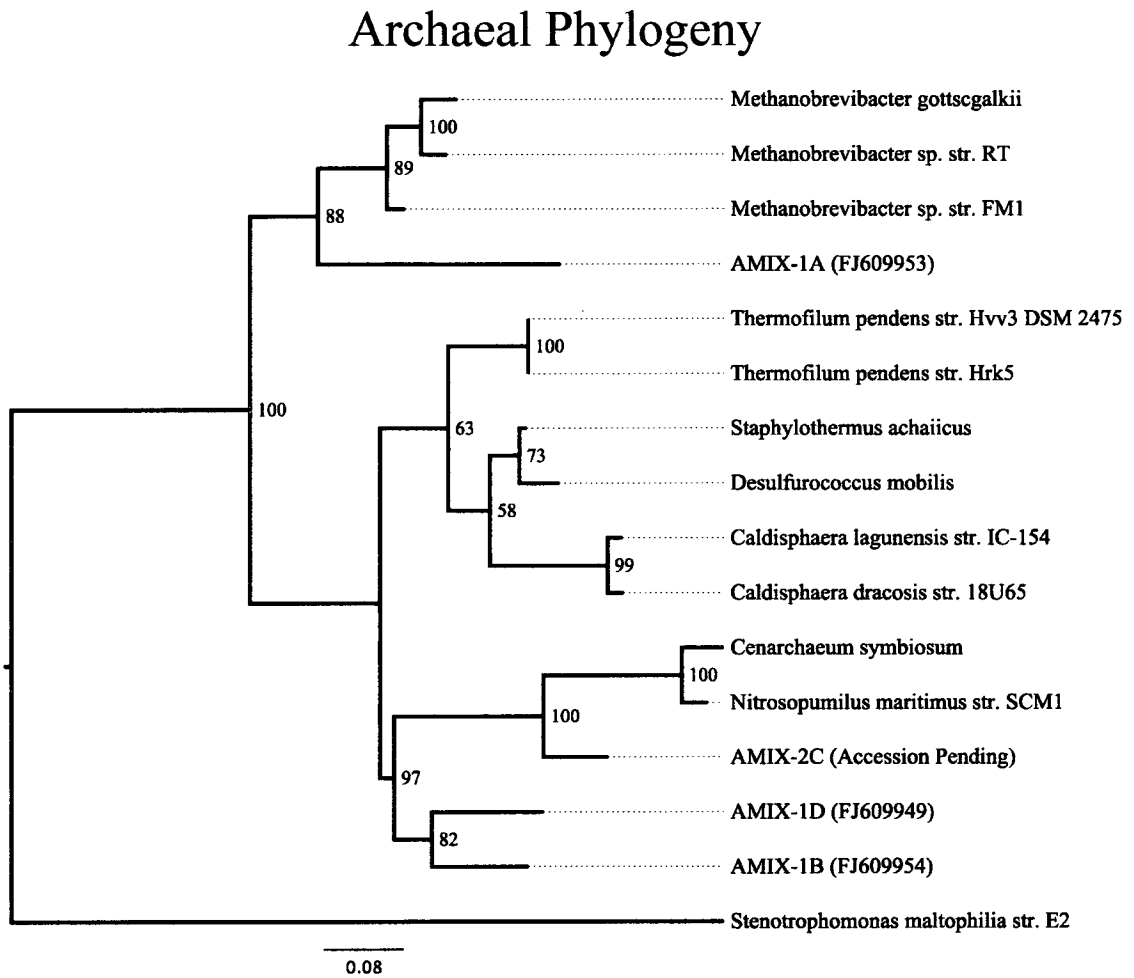

Figure 13. Archaeal Phylogeny. Maximum-likelihood phylogenetic tree of unknown archaeal clones alongside non-chimeric nearest neighbor isolates drawn from the NCBI and RDP databases by Simrank, an N-mer comparison tool. The Gammaproteobacterium Stenotrophomonas maltophilia str. E2 (AY841799.1) served as the outgroup. Numbers in parenthesis following the isolate name refer to the GenBank accession numbers. Maximum likelihood bootstrap values (100 resamplings) of >50% are shown on branches in boldface. Node value are bootstrapped neighbor joining distance grouping percentages (1,000 resamplings).

Thirty-two bacterial clones were sequenced, two of which were identified as Archaea. Of the 30 remaining sequences, similarity analysis indicated that seven were duplicates (<1% different) leaving 25 unique bacterial sequences (Figure 9). Fifteen of these sequences were isolated from depths at or below 100 cmbsf and are considered members of the shallow consortia. Ten sequences were isolated from 126 cmbsf and are considered members of the deep consortia. The results from The National Center for Biotechnology Information's (NCBI's) Basic Local Alignment Search Tool (BLAST) are presented here (Figure 10). Two bacterial maximum likelihood trees are illustrated. The first is a phylogram and depicts genetic distances (Figure 11). The second is a cladogram and allows space for maximum parsimony bootstrap values (n=10,000) (Figure 12).

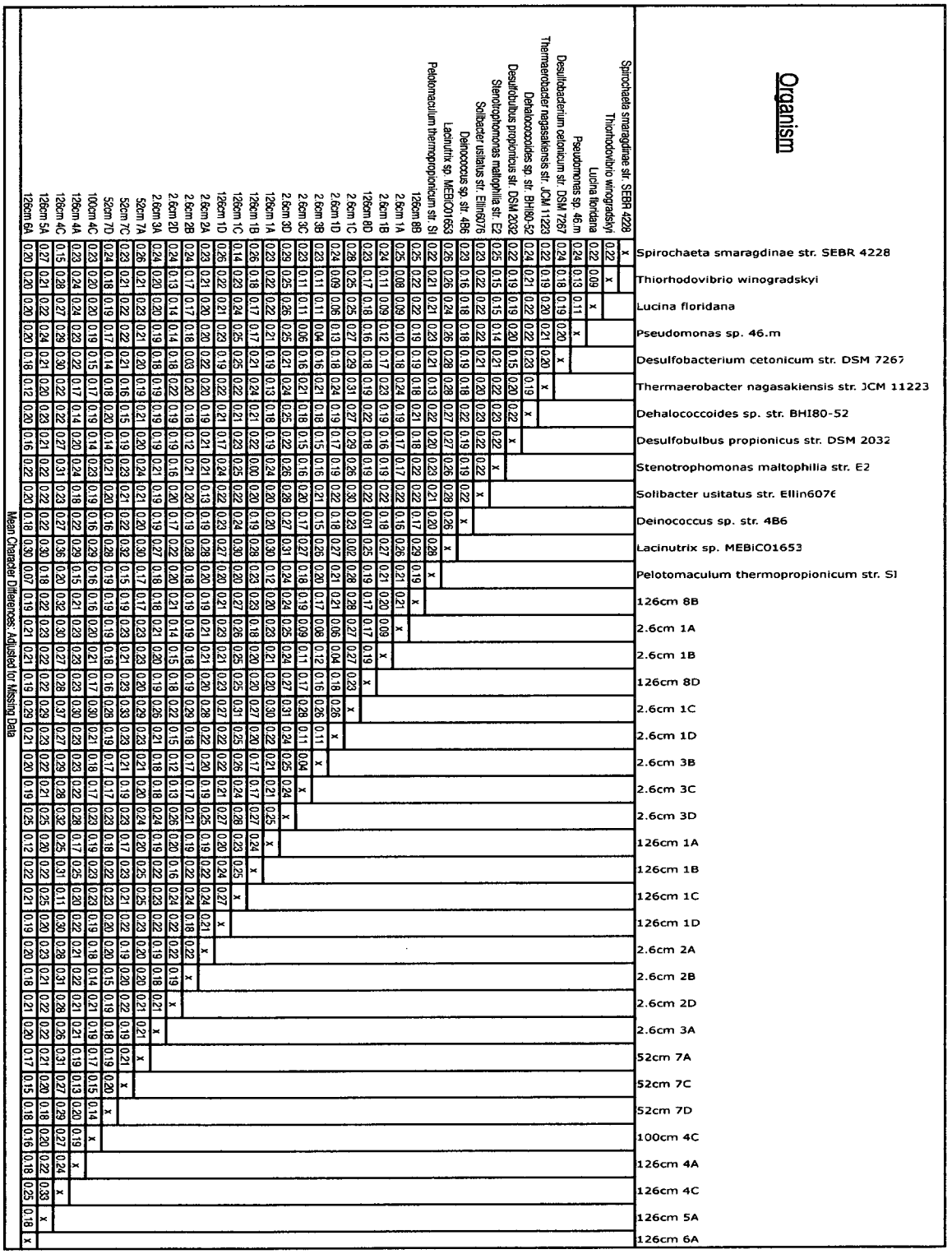

Figure 14. 16s rRNA Gene Sequence Similarity Matrix for Bacteria.

Domain	DGGE Band no.	Phylogenetic Group	Closest Relative (NCBI)	Percent Similarity	GenBank Accession no.
Archaea					
	AMIX-1B	*Crenarchaeota*	Uncultured Archaeon clone ZES-75	94%	EF367512.1
	AMIX-1D	*Crenarchaeota*	Uncultured *Crenarchaeote* clone kLNP Ar 2	90%	AY731480
	AMIX-2C	*Crenarchaeota*	Uncultured Archaeon clone ZES-215	99%	EF367652
	AMIX-1A	*Euryarchaeota*	Uncultured Archaeon clone SBAK-deep-27	97%	DQ640146.1
Bacteria					
	2.6 cm-1A	*Gammaproteobacteria*	Uncultured *Chromatiales* bacterium	95%	AM501811
	2.6 cm-1B	*Gammaproteobacteria*	Uncultured bacterium clone Amsterdam-1B-19	95%	AY592324.1
	2.6 cm-1C	*Bacteroidetes*	*Flavobacteriaceae* bacterium A2	98%	FJ348469
	2.6 cm-1D	*Gammaproteobacteria*	Uncultured bacterium clone Amsterdam-1B-19	98%	AY592324.1
	2.6 cm-2A	*Acidobacteria*	Uncultured bacterium clone B8S-122	95%	EU652508.1
	2.6 cm-2B	*Deltaproteobacteria*	Uncultured *Deltaproteobacteria*	99%	AM882640.1
	2.6 cm-2D	*Gammaproteobacteria*	Uncultured *Gammaroteobacteria*	97%	AM882548
	2.6 cm-3A	*Actinobacteria*	Uncultured *Actinobacterium* clone JBS 8206	99%	EU702795
	2.6 cm-3B	*Gammaproteobacteria*	Uncultured *Gammaroteobacteria* clone MSB-4F10	98%	DQ811844
	2.6 cm-3C	*Gammaproteobacteria*	Uncultured bacterium clone C8S-46	97%	EU652529
	2.6 cm-3D	*Verrucomicrobiae*	Uncultured Verrucomicrobiae clone NdGall	99%	FJ752762
	52 cm-7A	*Deltaproteobacteria*	Uncultured bacterium clone MD2894-B35	95%	EU386029
	52 cm-7C	*Chloroflexi*	Uncultured bacterium clone 10bav C11red	95%	EU181504
	52 cm-7D	*Deltaproteobacteria*	Uncultured *Geobacter* sp. clone VHS-B3-70	99%	DQ394958
	100 cm-4C	*Deltaproteobacteria*	Uncultured *Deltaproteobacteria* clone MSB-3A9	98%	DQ811792
	126 cm-1A	*Firmicutes*	Uncultured bacterium gene	94%	AB300079
	126 cm-1B	*Gammaproteobacteria*	*Stenotrophomonas maltophilia* strain SPd	100%	FJ405363
	126 cm-1C	*Spirochaetes*	Uncultured *Spirochete* clone IE073	92%	AY605143
	126 cm-1D	*Deltaproteobacteria*	Uncultured bacterium	91%	AM943592
	126 cm-4A	*Chloroflexi*	Uncultured *Chloroflexi* bacterium	97%	AB448868
	126 cm-4C	*Spirochaetes*	Uncultured bacterium gene	96%	AB177319
	126 cm-5A	*Deltaproteobacteria*	Uncultured bacterium gene	95%	AB300123
	126 cm-6A	*Firmicutes*	Uncultured *Peptococcaceae* bacterium clone ORCL4.4	95%	EF042587
	126 cm-8B	*Actinobacteria*	Uncultured *Actinobacterium* clone AT s3-3	94%	AY225602
	126 cm-8D	*Alphaproteobacteria*	*Methylobacteriaceae* bacterium RCML-7	99%	FJ005068

Figure 15. National Center for Biotechnology Information's (NCBI's) Basic Local Alignment Search Tool (BLAST) Results.

Bacterial Phylogeny

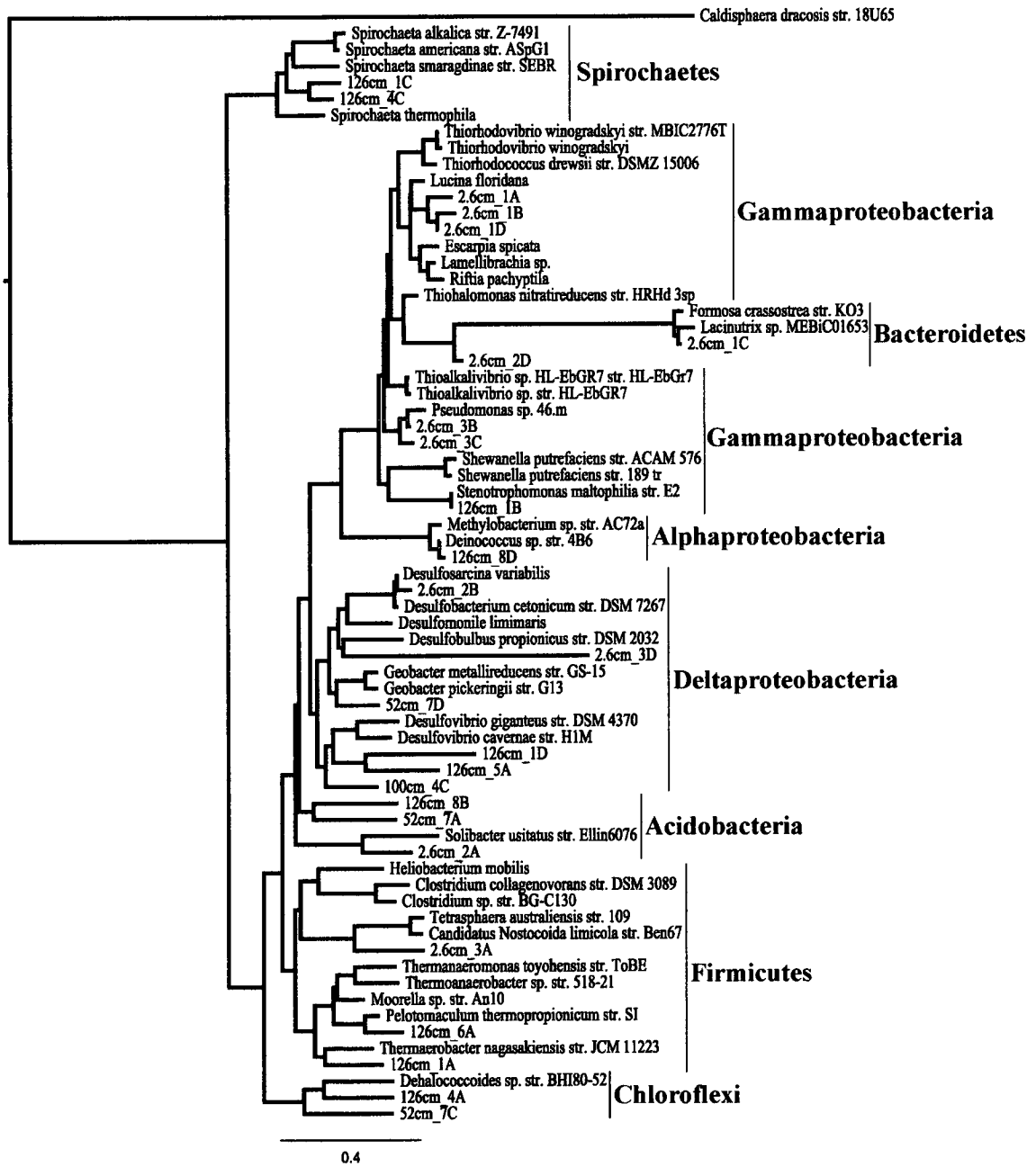

Figure 16. Bacterial Phylogeny. Maximum-likelihood phylogenetic tree of unknown bacterial clones alongside non-chimeric nearest neighbor isolates drawn from the NCBI and RDP databases by Simrank, an N-mer comparison tool. The archaeon Caldisphaera dracosis str. 18U65 served as the outgroup.

Bacterial Equal Branch Length Phylogenetic Tree

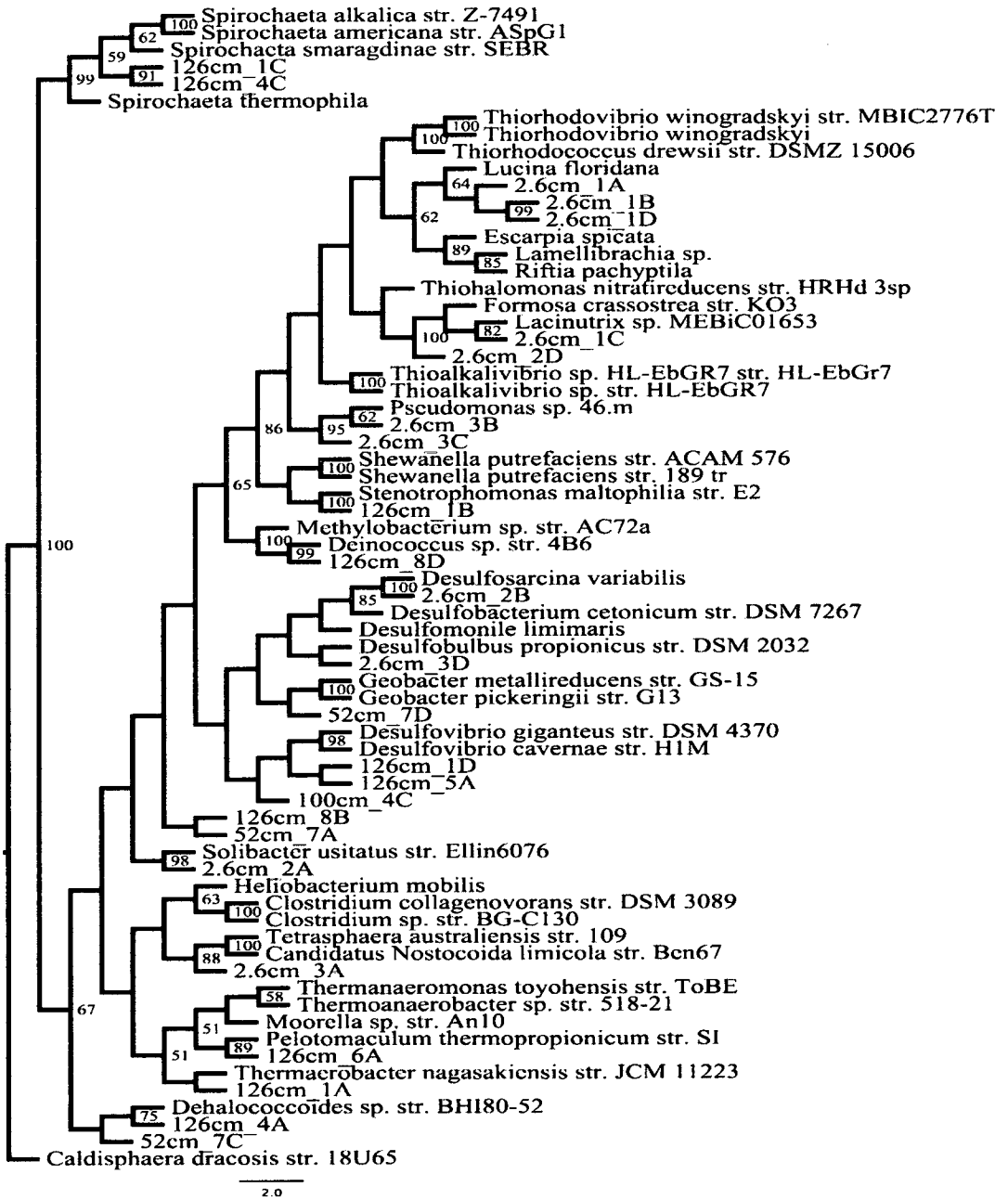

Figure 17. Bacterial Equal Branch Length Phylogeny. Maximum-likelihood equal branch length phylogenetic tree of unknown bacterial clones alongside non-chimeric nearest neighbor isolates drawn from the NCBI and RDP databases by Simrank, an N-mer comparison tool. The archaeon Caldisphaera dracosis str. 18U65 served as the outgroup. Branch labels are maximum parsimony bootstrap values (n=10,000).

Maximum-likelihood phylogenetic analysis of the 16S rRNA gene on forty-two known bacterial taxa and twenty-five Hudson's Landing samples identified nine lineages with mixed statistical support (Figures 15, 16). The most basal of these lineages was the *Spirochaetes* (BP=99), which contained samples 126cm-1C and 126cm-1D. The remaining taxa were grouped in a moderately supported clade (BP=67). Of these, the *Chloroflexi* included samples 52cm-7C and 126cm-4A. The *Firmicutes*, although weakly supported, formed an assemblage with slough samples 126cm-1A, 126cm-6A, and 126cm-3A. Sister to this is a well-supported clade (BP=98) containing sample 2.6cm-2A and *Solibacter usitatus*, an *Acidobacterium*. Samples 126cm-8B and 52cm-7A grouped together in a poorly supported clade basal to another unsupported clade representing the *Deltaproteobacteria* containing samples 2.6cm-2B, 2.6cm-3D, 52cm-7D, 126cm-1D, 126cm-5A, and 100cm-4C. The remaining taxa were grouped in a moderately supported clade (BP=65) with two lineages. One well-supported lineage represents the *Alphaproteobacteria* (BP=100) and contains sample 126cm-8D. The second lineage is also well supported (BP=86) and represents *Bacteroidetes* and *Gammaproteobacteria*. Sequences 2.6cm-1C and 2.6cm-2D, representing *Bacteroidetes,* formed a well-supported clade (BP=100) within the larger assemblage of sequences representing *Gammaproteobacteria*. Within the *Gammaproteobacteria*, sample 126cm-1B formed a well-supported clade (BP=100) with *Stenotrophomonas maltophilia*, while samples 2.6cm-3C and 2.6cm-3B formed a well-supported clade (BP=95) with *Pseudomonas*. Samples 2.6cm-1A, 2.6cm-1B, and 2.6cm-1D were grouped in a moderately supported (BP=62) clade containing sulfur-oxidizing endosymbiotic *Gammaproteobacteria*.

Discussion

Prokaryotes play critical and fundamental roles in estuarine nutrient cycling, yet their ecology is not well understood. This study identifies a shift in the microbial consortia present at 100 cmbsf in estuarine sediment at Hudson's Landing in Elkhorn Slough. Hudson's Landing is a depositional region, and carbon-14 dates from nearby cores suggest a depositional rate of approximately 1mm/yr (E. Watson: personal communication). The data presented in this study were taken from a 1.26 m core representing an estimated 1,260 years of deposition.

In 2002 and 2003, Jane Caffrey published the following biogeochemical data collected at the Hudson's Landing study site (Caffrey et al., 2002; Caffrey et al., 2003). These data allow biogeochemical comparisons to be made both between different sites in Elkhorn Slough and between Hudson's Landing and sites in estuaries elsewhere. Between November 1997 and December 1999, the temperature of the overlying water ranged from approximately 10°C to 25°C. Salinity values ranged from 0 ‰ (El Nino runoff event) to 36 ‰ with oxygen concentrations never dropping below 62.5 μM/L. Water column nitrite and nitrate concentrations were inversely correlated with salinity and positively correlated with precipitation. Values were typically above 50 μM. Ammonium concentrations were usually above 3 μM with a peak greater than 30 μM in the summer of 1998. Dissolved inorganic phosphate (DIP) values were highest following agricultural runoff events in the late summer and exceeded 15 μM.

Hudson's Landing surface sediment is 76% water (SE=2) with an organic content of 17% (SE=2) (Caffrey, 1996). Pore water NH_4^+, DIP, and S^{2-}concentrations in the

upper 3 cm of sediment always increased with depth and generally peaked during the summer (Caffrey et al., 2002; Caffrey et al., 2003). NH_4^+ readings exceeded 1500 μM at 3 cm in July 1999. DIP values topped 100 μM, and S^{2-} levels were higher than 150 μM. Sediment oxygen consumption (SOC) rates ranged from 24.2-107.5 mmol $m^{-2}d^{-1}$ with a measured diffusive O_2 flux of 23 mmol $m^{-2}d^{-1}$. Microelectrode measurements indicate 0.9 mm of dissolved O_2 penetration into these sediments. These flocculent sediments very rapidly become anoxic due to the carbon load resulting in very narrow geochemical gradients. Metabolic products from one geochemical region can easily diffuse into an adjoining region facilitating syntrophic relationships.

Nitrification rates can be reduced by high salinity, high pore-water sulfide, and low dissolved oxygen (Caffrey, Bano, Kalanetra, and Hollibaugh, 2007). Despite high pore water sulfides and anoxic sedimentary conditions occurring within 1 cm of the sediment surface, Hudson's Landing's surficial sediment boasts nitrification rates among the highest reported in the literature (Caffrey et al., 2002; Caffrey et al., 2003). Caffrey recorded nitrogen mineralization rates of 9.2 mmol $m^{-2}d^{-1}$ and a denitrification rate of 4.6 mmol $m^{-2}d^{-1}$, meaning that 50% of the mineralized nitrogen was coupled to denitrification at this site. While nitrification requires an oxidizing environment, denitrification is not energetically favored under oxic conditions. Hudson's Landing sediment has an oxygen gradient measured in micrometers with strongly reducing sediments immediately beneath the sediment-water interface.

The measured range of ORP values (-150 to -175mV) and moderate pH (7.25 to 8.25) make possible a diverse range of metabolic processes (Weiner, 2000).

Denitrification is favored at pH values ranging from 6.2 to 10.2 and at ORP values ranging from -200 mV to 665 mV. Sulfate reduction is favored at pH 7 and ORP of approximately -200 mV. Methanogenesis is favored at pH 7 and ORP greater than −200 mV. Given the presence of microenvironments in the sedimentary matrix and the diversity of microbes isolated from this environment, it is reasonable to assume that a wide variety of metabolic processes occur in Elkhorn Slough sediment.

The effective sedimentary surface area is further increased by bioturbators, such as the tubeworms that dominate the benthos, and the formation of microenvironments inside of fecal pellets and other bits of organic matter. It is thought that the composition of these nitrifying bacterial communities changes within the slough both seasonally and spatially and is determined by nutrient concentrations of the source water (Caffrey et al., 2002; Caffrey et al., 2003). Any change in the hydrology of the slough resulting in anoxic bottom conditions could dramatically affect nitrification rates in the surface sediments.

The sediment's surface was covered with small tubeworms. Amphipods and copepods were observed in the overlying water. The pressure of the core liner on the sediment during coring forced small bubbles out of the sediment. The gas smelled like hydrogen sulfide and, while it likely contained some methane due to the presence of methanogens and methanotrophs in the sediment, captured bubbles were not at a high enough concentration to ignite indicating a methane concentration of greater than 4.6% (Cashdollar, Zlochower, Green, Thomas, and Hertzberg, 2000).

These tubeworms are bioturbators and their tubes were observed to a depth of

approximately 10 cmbsf. Because the overlying water at Hudson's landing never goes completely anoxic, these worms continually cycle oxygenated water into the otherwise anoxic sediment increasing the surface area of the sediment that is aerated, if only to a depth of a few hundred microns, thereby increasing nitrification rates. This thin layer of oxygenated sediment is important because nitrifying bacteria and Archaea require oxygen to oxidize ammonium, which might otherwise contribute to eutrophication, to nitrite and nitrate that can then be denitrified back to nitrogen gas, which re-enters the atmosphere. Recent data suggests that marine *Crenarchaeota*, found in Hudson's Landing sediment, play a major role in oceanic nitrification rates (Wuchte, Abbas, Coolen, 2006). Rapid erosion and/or deposition could disturb these gradients and effect the coupling of denitrification to nitrification rates in Elkhorn Slough.

In addition to nitrification, anaerobic methane oxidation is an ecologically important microbially mediated reaction occurring in estuarine sediments. The reaction is as follows: $CH_4 + SO_4^{2-} \rightarrow HCO_3^- + HS^- + H_2O$. Anaerobic methanotrophs are responsible for oxidizing the majority of methane produced in anoxic sediments (Roden and Wetzel, 1996), thereby mitigating greenhouse gas emissions, and the hydrogen sulfide that is produced as a byproduct can be utilized by sulfide oxidizers found throughout the core. Methanotrophic bacteria oxidize methane to carbon dioxide and produce hydrogen gas. They are known to exist symbiotically with sulfate reducing bacteria that reduce the hydrogen gas to protons that are subsequently used by fermentative bacteria (Hoehler, Alperin, and Martens, 1994). More recently, anaerobic methane oxidation has also been tied to the reduction of nitrate (Raghoebarsing, Pol, van

de Pas-Schoonen, 2006).

The observed shift at Hudson's Landing can be described as a change from surface sediments dominated by *Proteobacteria* (73%) to deeper sediments where they were not as abundant (40%). In the deep group there was no one taxon that dominated although representatives of the phyla *Spirochaeta* and *Firmicutes* appeared for the first time and several sequences were closely related to *Chloroflexi, Peptococcaceae,* and *Halanaerobiales*. These prokaryotes are capable of using diverse fermentative metabolic pathways to oxidize degradation products of the breakdown of macromolecules. Phenotypic suggestions based on the genotype of a portion of the 16S rRNA gene are made with caution. A separate study in Elkhorn Slough found an isolate capable of oxidizing Mn(II) to Mn(III,IV) oxides that is 100% similar at the 16S rRNA gene level to a previously described *Pfiesteria*-associated *Roseobacter*-like bacterium that is incapable of Mn oxidation (Hansel and Francis, 2006).

The largest number of clones from any bacterial phylum came from the group *Proteobacteria*. Of the thirteen clones, eleven came from samples taken above the community shift at 100 cmbsf and four came from the deepest sample. Of the eleven from the surface sample, six were *Gammaproteobacteria*, four were *Deltaproteobacteria,* and one was an *Alphaproteobacteria*. The *Gammaproteobacteria* are a phenotypically diverse group of bacteria that are phylogenetically very closely related. The shallow clones from this class fell into two distinct groups. 2.6cm-1A, 2.6cm-1B, and 2.6cm-1D formed a phylogenetic clade within a larger clade consisting of *Lucina floridana, Escarpia spicata, Lamellibrachia sp.,* and *Riftia pachyptila*. The phylogeny of *E.*

spicata, Lamellibrachia sp. and *R. pachyptila*, all sulfur oxidizing vestimentiferan endosymbionts, can be found here (Duhaime, 2003). *L. floridana* is an endosymbiont as well, but is associated with a bivalve found in eelgrass beds overlying sulfide–rich sediments (Fisher and Hand, 1984). As the Hudson's Landing study site is covered with tubeworms, it is conceivable that these sequences are derived from an endosymbiont of these worms, although further study is necessary to confirm this hypothesis.

The second group of *Gammaproteobacteria* from the shallow community consisted of clones 2.6cm-3B and 2.6cm-3C that are 96%, 94% similar to *Pseudomonas* sp. 46.m. *Pseudomonas*, first named in 1894, are an order of gram-negative rod-shaped bacteria that were thought to consist exclusively of obligate aerobes capable of respiring organic material using nitrate as a terminal electron acceptor, although it now appears that at least one biofilm forming class is capable of anaerobic respiration (Hassett, Cuppoletti, Trapnell, 2002). They are common in sediments and soils (Knowles, 1982). BLAST results indicate that these clones were closely related to uncultured clones obtained from sediment samples.

The first of the four shallow clones falling into the class *Deltaproteobacteria*, 2.6cm-2B, was closely related (99%) to *Desulfosarcina*, a sulfate reducing bacteria associated with methanotrophs (Treude, Orphan, Knittel, 2007). The abundance of sulfate in shallow marine sediments combined with previously reported ORP measurements suggested the presence of sulfate reducers. The second clone, 2.6cm-3D, also fell within the clade of sulfate-reducing bacteria, however BLAST results indicate that it is likely a member of the phylum *Verrucomicrobiae*. A new species was recently

identified that is capable of methane oxidation in oxygen limiting environments (Pol, Heijmans, Harhangi, 2007). The third clone, 52cm-7D, is most closely related to *Geobacter metallireducens* (89%). This bacterium is the first organism found capable of oxidizing hydrocarbons to carbon dioxide with iron oxides as the electron acceptor and has potential for use in bioremediation of radioactive metals and in the generation of electricity (Methe, Nelson, Eisen., 2003). The fourth clone, 100cm-4C, grouped with two clones from the deep community (126cm-1D and 126cm-5A). It's nearest neighbors, the slightly halophilic *Desulfovibrio giganteus* (Esnault, Caumette, and Garcia, 1988) and *Desulfovibrio cavernae* (Sass and Cypionka, 2004), are gram negative sulfate reducing bacteria common in organic-rich aquatic environments. Members grouping within the *Desulfovibrio* clade were detected in both the shallow and deep communities, indicating that sulfate reduction was occurring both above and below the 100 cmbsf horizon. This observation helps explain the constant ORP profile across the community break.

Two clones from the shallow community grouped within the phylum *Bacteroidetes*. The closest neighbors to clone 2.6cm-1C were *Lacinutrix* sp. MEBiCo1653 (98%) and *Formosa crassostrea* (98%). Both are members of the class *Flavobacteriaceae* which contains more than 20 genera of ubiquitous bacteria thought to degrade complex polysaccharides and other biomacromolecules (Ivanova, Alaxeeva, Flavier, 2004). These bacteria are common in environmental samples and are often opportunistic pathogens. Clone 2.6cm-2D is 97% similar to an uncultured *Gammaproteobacterium* and is most similar to isolates of the purple-sulfur bacteria *Chromatiales*, which are known sulfide oxidizers (Imhoff, 2008).

The remaining sequences isolated from the shallow community were from the phyla *Acidobacteria, Actinobacteria,* and *Chloroflexi*. Clone 2.6cm-2A is 87% similar to the Acidobacterium *Solibacter usitatus* str. Ellin6076. Despite being ubiquitous in sediment and forming a coherent phylogenetic phylum, the metabolic capabilities of *Acidobacteria* are poorly understood (Quaiser, Ochsenreiter, Lanz, 2003). Recent work indicates that they are capable oxidizing a wide variety of carbon substrates from simple sugars to cellulose and chitin, by reducing nitrate and nitrite (Ward, Challacombe, Janssen, 2009). Clone 2.6cm-3A is in the phylum *Actinobacteria* and is most closely related to *Streptomyces coelicolor* A3(2) (87%). *S. coelicolor* A3(2) is a soil-dwelling, filamentous bacteria, with broad metabolic capabilities whose genome contains 7,825 genes including more than 20 clusters coding for known or predicted secondary metabolites (Bentley, Chater, Cerdeno-Tarraga, 2002). It is now clear that marine *Actinobacteria* are a source of many novel compounds that will likely be a source of new medicines (Jensen, Mincer, Williams, and Fenical, 2004). Clone 52cm-7C, phylum *Chloroflexi*, was 85% similar to *Dehalococcoides* sp. str. BHI80-52. *Dehalococcoides* is a genus of bacteria that oxidize hydrogen gas and reduce halogenated organic compounds such as soil-contaminant tetrachloroethylene (Maymo-Gatell, Chien, Gossett, and Zinder, 1997).

The deep community was more diverse with not more than two sequences belonging to any one phylum. The two deep *Deltaproteobacteria* clones, 126cm-1D and 126cm-5A, were 81% and 80% similar to clone 100cm-4C. These clones also shared the same nearest neighbors: the sulfate reducing *Desulfovibrio giganteus* and *Desulfovibrio*

cavernae described above. Clone 126cm-8B was 83% similar to clone 52cm-7A and 81% similar to clone 2.6cm-2A and shared the nearest neighbor *Solibacter usitatus* str. Ellin6076. The deep clone 126cm-4A is 87% similar to clone 52cm-7C and 86% similar to *Dehalococcoides* sp. str. BHI80-52. The ecology of this bacterium is described above. All other clones from the deep community were distinct from any sequences found in the shallow community.

The deep community clone 126cm-1B was 100% similar to *Stenotrophomonas maltophilia*. *S. maltophilia* is an aerobic, non-fermentative, Gram-negative bacterium with high interspecies diversity (Berg, Roskot, and Smalla, 1999). In phylogenetic studies, environmental isolates did not cluster separately from the clinical samples and were highly resistant to antibiotics (Berg et al., 1999). Their aerobic nature makes it likely that either they are inactive at 126 cmbsf or that the sequence is from an anaerobic strain that is 100% similar to *S. maltophilia* across the 16S gene.

Clones 126cm-1C and 126cm-4C were 86% and 85% similar to *Spirochaeta smargdinae* str. SEBR 4228. *Spirochaetea*, as a phylum, are tolerant of a wide range of oxygen levels and may play a role in the cycling of sulfur in microbial mat consortia by oxidizing sulfide, thereby promoting the activity of sulfate reducing bacteria (Stephens, Braissant, and Visscher, 2008). Their mobility may allow them to migrate towards a depth horizon where both sulfide and a suitable electron acceptor (oxygen or nitrate) exist (Kamp, Stief, and Schulz-Vogt, 2006). Their absence from the shallow community is conspicuous and they may be out-competed by other bacterial and archaeal sulfide oxidizers such as *Desulfurococcus, Chromatiales,* or the sulfur-oxidizing endosymbionts.

One clone detected in the deep community, 126cm-8D, is 98% similar to *Methylobacterium sp. Str. AC72a*, an *Alphaproteobacterium*. *Methylobacterium* sp. are methanotrophs known to oxidize methane in wetland rice fields (Eller and Frenzel, 2001). Considered aerobic, *Methylobacter sp.* are capable of limited metabolism under anaerobic starvation conditions (King, 1995).

Within the phylum *Firmicutes,* Clone 126cm-6A was 95% similar to *Peptococcaceae* gen. which are capable of fermenting protein degradation products resulting in the production of carbon dioxide and hydrogen gas (Rogosa, 1971). Clone 126cm-1A groups with members of the genus *Thermoaerobacter* within the anaerobic class *Clostridia*. Another member of this class isolated from tidal flat sediment is described as a strictly anaerobic, halophilic, motile, endospore-forming rod-shaped bacterium that ferments glucose and produces butyric acid, propionic acid, glycerol, and dihydrogen gas (Kim, Jeong, and Chun, 2007).

Deep-biosphere communities have been characterized by a shift from *Proteobacteria* dominated sediments to sediments dominated by *Chloroflexi* (Coolen, Cypionka, Sass, 2002; Inagaki, Suzuki, Takai, Oida, Sakamoto, Aoki, 2003; Kormas, Smith, Edgcomb, and Teske, 2003). Construction of a more comprehensive clone library is required to accurately quantify the relative abundance of various phyla, however bacterial sequences 126cm-4A and 52cm-7C are 86% and 85% similar to *Chloroflexi Dehalococcoides sp.* which is known to degrade tetrachloroethene, a highly refractory substance, using hydrogen as an electron donor (Seshadri, Adrian, Fouts, Eisen,

Phillippy, and Methe, 2005). The connection between deep-biosphere *Chloroflexi* communities and *Chloroflexi* communities found in estuarine sediment has been observed in the Wadden Sea (Wilms et al., 2006a). Observations of *Dehalococcoides* related bacteria in Elkhorn Slough sediment support these observations and suggest that deep-biosphere related communities may be ubiquitous in estuarine sediment

Conclusion

The first insights into the bacterial consortia in deeper tidal-flat sediments took place in the Wadden Sea and revealed a shift from *Proteobacteria* to *Firmicutes* with depth (Kopke, Wilms, Engelen, Cypionka, and Sass, 2005). This study supports the observations made in the Wadden Sea suggesting that this pattern may be ubiquitous. A study comparing bacterial consortia in estuaries to consortia found living in similar thermodynamic conditions in the deep sub-seafloor found a shift from *Proteobacteria* dominated sediments to *Chloroflexi* dominated sediments with depth (Wilms et al., 2006a). This finding suggests that further study of estuarine sediment can provide information about the deep-biosphere that may contain 1.3×10^{29} prokaryotic cells and 2.5×10^{15} g of carbon (Schippers et al., 2005). This number represents more than half of the total prokaryotic cells on Earth.

Syntrophic relationships dominate in the sediment column (Figure 13). For example, sulfate reducers convert sulfate to sulfide while oxidizing organic material. Sulfide oxidizers reduce oxygen and convert sulfide back to sulfate or sulfite. Methanogens reduce carbon dioxide to methane while methanotrophs metabolize methane as their carbon source by reversing the methanogens metabolic pathway. And, while fermentative bacteria are not strictly dependent on syntrophic relationships, they profit from the activity of hydrogen scavenging microbes as they gain maximum energy yield when protons are used as the electron acceptor resulting in the production of hydrogen gas. These symbiotic relationships are not easily inferred when the sediments are treated as a black box, as by definition only the inputs and exports are measured. An

estuarine management plan attempting to maximize beneficial microbial processes, (anaerobic oxidation of methane: a potent greenhouse gas) while minimizing those that are derogatory (methylation of mercury by sulfate reducing bacteria), should include a study of the local syntrophic consortia as it may be possible to get positive results by taking an ecosystem approach to managing inputs.

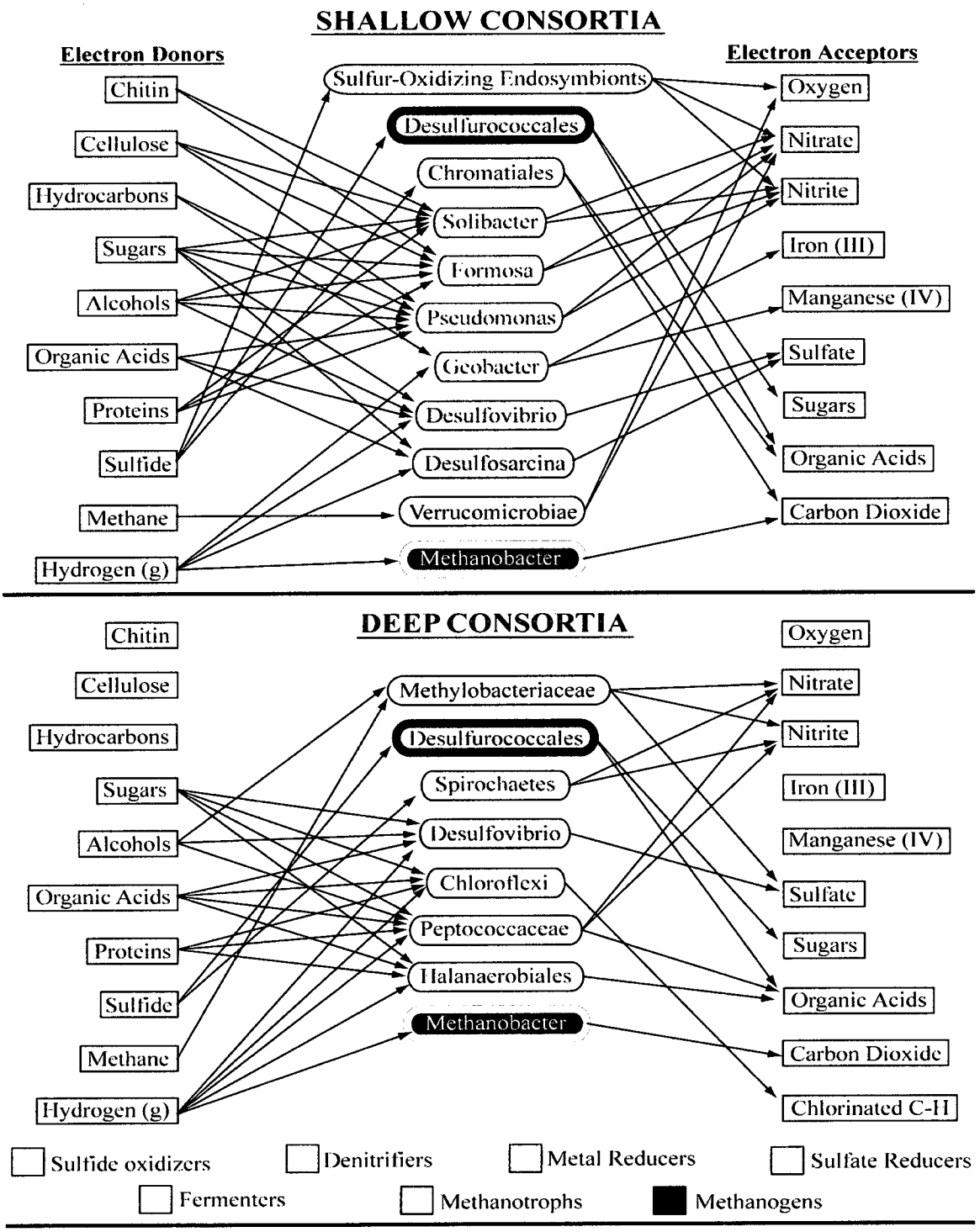

Figure 18. Prokaryotic Metabolisms in Shallow and Deep Communities. Representative members of the shallow and deep consortia are shown here alongside oxidized and reduced substrates. Archaeal representatives from Crenarchaeota (Desulfurococcales) and Euryarchaeota (Methanobacteria) are outlined. The arrows

represent the direction of reductive electron transfer. Many of these prokaryotes take advantage of a variety of electron donors and electron acceptors. The upper consortium is more diverse. There is evidence of active denitrifying communities (Solibacter, Formosa, Pseudomonas), iron reduction (Geobacter), and sulfate reduction (Desulfovibrio, Desulfosarcina) as would be expected in shallow estuarine sediment. There is a community of sulfide oxizers (Desulfurococcales, Chromatiales, endosymbionts) metabolizing the products of sulfate reduction. The archaeon Methanobacter is associated with Desulfosarcina and it's end product, methane, serves as the electron donor for the methanotrophic Verrucomicrobiae. The deep consortia is less diverse. While there is evidence of continued methanotrophy, sulfide oxidation, sulfate reduction, and methanogenesis, the denitrifying communities are replaced by a community of fermentative bacteria (Chloroflexi, Peptococcaceae, and Halanaerobiales).

There are notable differences between the bacterial metabolisms found in the shallow and deep consortia. The 16S rDNA gene sequence data from the shallow consortia show the presence of denitrifying bacteria and metal reducing bacteria that were not found in the deep consortia. The denitrifying bacteria are capable of oxidizing chitin, cellulose, and proteins as well as simple sugars and alcohols using either nitrate or nitrite as a terminal electron acceptor. Nutrient data show elevated nitrate and nitrite levels in the water column resulting from fertilizer runoff from nearby agricultural fields. Additionally, hydrocarbons are broken down in the surface sediments by bacteria using iron III and manganese IV as terminal electron acceptors.

The deep consortium is more specialized and more diverse with fermentative bacteria replacing the denitrifying and metal reducing bacteria. Below 100 cmbsf there were no bacteria detected capable of breaking down cellulose, chitin, or hydrocarbons. Smear slides and specific surface area measurements suggest that the organic carbon in the deeper sediment layer is derived largely from diatoms while the upper layer is primarily fecal pellets and cellulosic plant material. This allochthonous particulate

organic carbon (POC) is lower in nitrogen than autochthonous, algal derived POC. This transition is reflected in the C:N data as the relatively nitrogen-rich diatomaceous carbon causes decreasing C:N values below 100 cmbsf. The relatively protein and lipid rich diatom debris would initially support a "shallow consortium" type community. However, once the macromolecules had been degraded and the depositional environment had shifted, the diatom unit would have become isolated and only organisms capable of surviving at the thermodynamic limit could persist.

The decrease in magnetic susceptibility is explained by the increased diatomaceous sedimentary fraction. If the mineral contribution to the sedimentary matrix remains constant, an increase in the diatom fraction will weaken the magnetic susceptibility of the sediment. A decreasing C: N ratio is also expected when changing from a carbon source dominated by plant material (C: N > 20 due to high concentrations of cellulosic material) and one dominated by phytoplankton (C: N roughly 6 due to increased proteins) (Schulz and Zabel, 2006). Although decreasing C: N with depth can be associated with preferential use of labile organic compounds during early diagenesis, this is not likely to be the driving force at 1m. An estimated sedimentation rate of 1mm/yr suggests that benthic microbes have had 1,000 years to extract these compounds.

Diatoms have a much higher surface area than any mineral of equal diameter as a result of the texture of their frustules (Ransom, Kim, Kastner, and Wainwright, 1998). Increased surface area due to increased texture could provide refuge from grazers and provide relief, thereby helping the bacterium adhere to the particle. Increased surface area when combined with fine-grained sediment could dramatically increase the resident

microbial populations. In one study, particles between 3-10μm in diameter exhibited 22% coverage by bacteria, those from 10-40μm in diameter exhibited 5% coverage, and those from 40-140μm in diameter exhibited 2% coverage (Almeida and Alcantara, 1992). These size classes generally reflect the size of the three modes observed in the Hudson's Landing core.

In deep sea sediments, diatom rich lithographic units are associated with higher microbial activity based on higher cell counts and stimulated prokaryotic activity, as determined by thymidine incorporation and sulfate reduction assays (D'Hondt et al., 2004). By using luminosity as a proxy for carbonate, microbial populations have also been shown to vary within lithographic units at Milankovitch frequencies due to changes in organic carbon, porosity, and solid-phase electron acceptors (Aiello and Bekins, 2008). Additionally, diatom tests suggest a carbon source rich in nitrogen, phosphorous, aluminum, boron, iron, and other trace elements, and are potentially better able to support diverse microbial communities.

In conclusion, although the water column does not go completely anoxic, oxygen penetrates the sediment < 1mm. Bioturbators in the benthic layer mix oxygenated water throughout their burrows, which extended to approximately 10 cmbsf. A distinct shift in the bacterial consortia was detected by DGGE analysis between 100 and 126 cmbsf. While syntrophic relationships between species using a variety of electron acceptors persisted throughout, bacteria capable of degrading macromolecules were detected only in the shallow sediments. In the deeper sediments, as a function of time and carbon source, these macromolecules have largely been metabolized and fermentative bacteria

metabolize the products of degradation. Other work shows that community shifts of this kind exist both in tidal flat sediment in the Wadden Sea, and in the deep-biosphere. Coincident with this community shift was an increase in the diatomaceous sedimentary fraction, a decrease in the C: N ratio, a decrease in the magnetic susceptibility of the sediment, and increasing CDOM concentrations. The ORP did not change over this break. These observations represent a first look at the community composition of the sediment at Hudson's Landing in Elkhorn Slough. The complexity of the microbial universe far exceeds the complexity of the macro-biological universe, particularly with respect to metabolic potential. An understanding of the microbial consortia in estuarine sediments is important from an estuarine management perspective and, potentially, may provide insights into the ecology of the deep-biosphere.

References

Achtman, M., and Wagner, M. (2008) Microbial diversity and the genetic nature of microbial species. *Nature* **6**: 431-440.

Aiello, I.W., and Bekins, B. (2008) Milankovitch-scale correlations between deeply buried microbial populations and biogenic ooze lithology. *Unpublished Data.*

Almeida, M.A., and Alcantara, F. (1992) Bacterial colonization of seston particles in brackish waters (Ria de Aveiro, Portugal). *Marine Ecology Progress Series* **89**: 165-173. Baas Becking, L.G.M. (1934) Geobiologie of inleiding tot de milieukunde. In *W.P. Van Stockum & Zoon*: The Hague, Netherlands.

Beckman Coulter, I. (2003) LS13 320 Particle size analyzer manual PN 7222061A. In. Beckman (ed). Miami.

Bentley, S.D., Chater, K.F., Cerdeno-Tarraga, A.M., et al. (2002) Complete genome sequence of the model actinomycete Streptomyces coelicolor A3(2). *Nature* **417**: 141-147.

Berg, G., Roskot, N., and Smalla, K. (1999) Genotypic and phenotypic relationships between clinical and environmental isolates of *Stenotrophomonas maltophilia*. *Journal Clinical Microbiology* **37**: 3594-3600.

Caffrey, J.M. (1996) Effect of land-use practices on nutrient dynamics in subtidal estuarine sediments in Elkhorn Slough, CA. In: National Oceanic and Atmospheric Administration, Sanctuaries and Reserves Division.

Caffrey, J.M., Harrington, N., and Ward, B. (2002) Biogeochemical processes in a small California estuary. 1. Benthic fluxes and pore water constituents reflect high nutrient freshwater inputs. *Marine Ecology Progress Series* **233**: 39-53.

Caffrey, J.M., Harrington, N., Solem, I., and Ward, B. (2003) Biogeochemical processes in a small California estuary. 2. Nitrification activity, community structure and role in nitrogen budgets. *Marine Ecology Progress Series* **248**: 27-40.

Caffrey, J.M., Bano, N., Kalanetra, K., and Hollibaugh, J.T. (2007) Ammonia oxidation and ammonia-oxidizing bacteria and archaea from estuaries with differing histories of hypoxia. *International Journal for Microbial Ecology* **1**: 660-662.

Cashdollar, K.L., Zlochower, I.A., Green, G.M., Thomas, R.A., and Hertzberg, M. (2000) Flammability of methane, propane, and hydrogen gases. *Journal of Loss Prevention in the Process Industries* **13**: 327-340.

Coolen, M.J.L., Cypionka, H., Sass, A.M., et al. (2002) Ongoing modification of Mediterranean Pleistocene sapropels mediated by prokaryotes. *Science* **306**: 2216-2221.

D'Hondt, S.L., Jorgensen, B.B., Miller, D.J., et al. (2004) Distributions of microbial activities in deep subseafloor sediments. *Science* **306**: 2216-2221.

de Wit, R., and Bouvier, T. (2006) 'Everything is everywhere, but, the environment selects'; what did Baas Becking and Beijerinck really say? *Environmental Microbiology* **8**: 755-758.

Duhaime, M. (2003) Phylogenetics of vestimentiferan symbionts from Guaymas Basin using the 16S and RuBisCO genes. In. Moss Landing: The Monterey Bay Aquarium Research Institute.

Eller, G., and Frenzel, P. (2001) Changes in activity and community structure of methane-oxidizing bacteria over the growth period of rice. *Applied Environmental Microbiology* **67**: 2395-2403.

Engelen, B., and Cypionka, H. (2009) The subsurface of tidal-flat sediments as a model for the deep biosphere. *Ocean Dynamics* **59**: 385-391.

Esnault, G., Caumette, P., and Garcia, J.L. (1988) Characterization of *Desulfovibrio giganteus sp. nov.*, a sulfate-reducing bacterium isolated from a brackish coastal lagoon. *Systematic and Applied Microbiology* **10**: 147-151.

Falkowski, P.G., Fenchel, T., and Delong, E. (2008) The mIcrobial engines that drive Earth's biogeochemical cycles. *Science* **320**: 1034-1039.

Felsenstein, J. (1985) Confidence limits on phylogenies: An approach using the bootstrap. *Evolution* **39**: 783-791.

Finley, B. (2002) Global dispersal of free-living microbial Eukaryote species. *Science* **296**: 1061-1063.

Fisher, M.R., and Hand, S.C. (1984) Chemoautotrophic symbionts in the bivalve *Lucina floridana* from seagrass beds. *Biological Bulletin* **167**: 445-459.

Green, J.L., Bohannan, B.J.M., and Whitaker, R.J. (2008) Microbial biogeography: from taxonomy to traits. *Science* **320**: 1039-1043.

Hambrick III, G.A., DeLaune, R.D., and Patrick, W.H.J. (1980) Effect of estuarine sediment pH and oxidation-reduction potential on microbial hydrocarbon degradation. *Applied and Environmental Microbiology* **40**: 365-369.

Hansel, C.M., and Francis, C.A. (2006) Coupled photochemical and enzymatic Mn(II) oxidation pathways of a planktonic *Roseobacter*-like bacterium. *Applied Environmental Microbiology* **72**: 3543-3549.

Hassett, D.J., Cuppoletti, J., Trapnell, B., et al. (2002) Anaerobic metabolism and quorum sensing by Pseudomonas aeruginosa biofilms in chronically infected cystic fibrosis airways: rethinking antibiotic treatment strategies and drug targets. *Adv Drug Deliv Rev* **54**: 1425-1443.

Hoehler, T.M., Alperin, D.B., and Martens, C.S. (1994) Field and laboratory studies of methane oxidation in an anoxic marine sediment: evidence for a methanogen-sulfate reducer consortium. *Global Biogeochem. Cycles* **8**: 451-463.

Hughes, B., and Haskins, J. (2007) Elkhorn Slough national estuarine research reserve. *Unpublished Data.*

Imhoff, J., F (2008) Systematics of anoxygenic phototrophic bacteria. In *Sulfur metabolism in phototrophic organisms*. Hell, R., and al., e. (eds): Springer.

Inagaki, F., Suzuki, M., Takai, K., Oida, H., Sakamoto, T., Aoki, K., et al. (2003) Microbial communities associated with geological horizons in coastal subseafloor sediments from the sea of Okhotsk. *Applied Environmental Microbiology* **69**: 7224-7235.

Ivanova, E., P, Alaxeeva, Y., V., Flavier, S., et al. (2004) *Formosa algae* gen. nov., sp. nov., a novel member of the family *Flavobacteriaceae. International Journal of Systematic and Evolutionary Biology* **54**.

Jensen, P.R., Mincer, T.J., Williams, P.G., and Fenical, W. (2004) Marine actinomycete diversity and natural product diversity. *Antonie van Leeuwenhoek* **87**: 43-48.

Kamp, A., Stief, P., and Schulz-Vogt, H.N. (2006) Anaerobic sulfide oxidation with nitrate by a freshwater *Beggiatoa* enrichment culture. *Applied Environmental Microbiology* **72**: 4755-4760.

Kim, S., Jeong, H., and Chun, J. (2007) *Clostridium aestuarii sp. nov.*, from tidal flat sediment. *International Journal of Systematic Evolutionary Microbiology* **57**: 1315-1317.

King, R.P. (1995) Aerobic and anaerobic starvation metabolism in methanotrophic bacteria. *Applied and Environmental Microbiology* **61**: 1563-1570.

Knowles, R. (1982) Denitrification. *Microbiological Reviews* **46**: 43-70.

Konstantinidis, K.T., Ramette, A., and Tiedje, J.M. (2006) The bacterial species definition in the genomic era. *Philosophical Transactions of The Royal Society* **361**: 1929-2940.

Kopke, B., Wilms, R., Engelen, B., Cypionka, H., and Sass, H. (2005) Microbial diversity in coastal subsurface sediments: a cultivation approach using various electron acceptors and substrate gradients. *Applied and Environmental Microbiology* **71**: 7819-7830.

Kormas, K.A., Smith, D.C., Edgcomb, V., and Teske, A. (2003) Molecular analysis of deep subsurface microbial communities in Nankai Trough sediments (ODP Leg 190, Site 1176). *FEMS Microbiological Ecolology* **45**: 115-125.

Maymo-Gatell, X., Chien, Y.-t., Gossett, J.M., and Zinder, S.H. (1997) Isolation of a bacterium that reductively dechlorinates tetrachloroethene to ethene. *Science* **276**: 1568-1571.

Methe, B.A., Nelson, K.E., Eisen, J.A., et al. (2003) Genome of *Geobacter sulfurreducens*: metal reduction in subsurface environments. *Science* **302**: 1967-1969.

Papke, R.T., Ramsing, N.B., Bateson, M.M., and Ward, D.M. (2003) Geographical isolation in hot spring cyanobacteria. *Environmental Microbiology* **5**: 650-659.

Pol, A.P., Heijmans, K., Harhangi, H.R., et al. (2007) Methanotrophy below pH 1 by a new *Verrocomicrobia* species. *Nature* **2007/12/6/online**.

Posada, D. (2006) ModelTest Server: a web-based tool for the statistical selection of models of nucleotide substitution online. *Nucleic Acids Research* **34**: W700-W703.

Quaiser, A., Ochsenreiter, T., Lanz, C., et al. (2003) Acidobacteria form a coherent but highly diverse group within the bacterial domain: evidence from environmental genomics. *Molecular Microbiology* **50**: 563-575.

Raghoebarsing, A.A., Pol, A.P., van de Pas-Schoonen, K.T., et al. (2006) A microbial consortium couples anaerobic methane oxidation to denitrification. *Nature* **440**: 918-921.

Ransom, B., Kim, D., Kastner, M., and Wainwright, S. (1998) Organic matter preservation on continental slopes: importance of mineralogy and surface area. *Geochemica et Cosmochimica Acta* **62**: 1329-1345.

Roden, E.E., and Wetzel, R.G. (1996) Organic carbon oxidation and suppression of methane production by microbial Fe(III) Oxide reduction in vegetated and unvegetated freshwater wetland sediments. *Limnology and Oceanography* **41**: 1733-1748.

Rogosa, M. (1971) *Peptococcaceae*, a new family to include the gram-positive, anaerobic cocci of the genera *Peptococcus, Peptostreptococcus,* and *Ruminococcus*. *International Journal of Systematic Bacteriology* **21**: 234-237.

Sass, H., and Cypionka, H. (2004) Isolation of sulfate-reducing bacteria from the terrestrial deep subsurface and description of *Desulfovibrio cavernae sp. nov.* *Systematic and Applied Microbiology* **27**: 541-548.

Schippers, A., Neretin, L.N., Kallmeyer, J., et al. (2005) Prokaryotic cells of the deep sub-seafloor biosphere identified as living bacteria. *Nature* **433**: 861-864.

Schulz, H.D., and Zabel, M. (2006) *Marine Geochemistry*: Birkhauser.

Schwartz, D.L., Mullins, H.T., and Belknap, D.F. (1986) *Holocene geologic history of a transform margin estuary: Elkhorn Slough, Central California.* London: Academic Press Inc.

Seshadri, R., Adrian, L., Fouts, D.E., Eisen, J.A., Phillippy, A.M., and Methe, B.A. (2005) Genome sequence of the PCE-dechlorinating bacterium *Dehalococcoides ethenogenes*. *Science* **307**: 105-108.

Stephens, E.A., Braissant, O., and Visscher, P.T. (2008) Spirochetes and salt marsh microbial mat geochemistry: Implications for the fossil record. *Carnets de Géologie / Notebooks on Geology* **Article 2008/09**: CG2008_A2009.

Strom, S.L. (2008) Microbial ecolgy of ocean biogeochemistry: a community perspective. *Science* **320**: 1043-1045.

Swofford, D.L. (2002) PAUP*. Phylogenetic Analysis Using Parsimony (*and Other Methods). In. Sunderland, MA: Sinauer Associates.

Treude, T., Orphan, V., Knittel, K., et al. (2007) Consumption of methane and CO2 by methanotrophic microbial mats from gas seeps of the anoxic Black Sea. *Applied and Environmental Microbiology* **73**: 2271-2283.

Ward, N.L., Challacombe, J.F., Janssen, P.H., et al. (2009) Three genomes from the phylum *Acidobacteria* provide insight into their lifestyles in soils. *Applied Environmental Microbiology* **7**: 2046-2056.

Weiner, E.R. (2000) *Applications of environmental chemistry: a practical guide for environmental professionals*: CRC Press.

Whitaker, R.J., Grogan, D.W., and Taylor, J.W. (2003) Geographic barriers isolate endemic populations of hyperthermophilic Archaea. *Science* **301**: 976-978.

Whitfield, J. (2005) Biogeography: is everything everywhere? *Science* **310**: 960-961.

Wilms, R., Kopke, B., and Sass, H. (2006a) Deep biosphere-related bacteria within the subsurface of tidal flat sediments. *Environmental Microbiology* **8**: 709-719.

Wilms, R., Sass, H., Kopke, B., Koster, J., Cypionka, H., and Engelen, B. (2006b) Specific bacterial, archaeal, and eukaryotic communities in tidal-flat sediments along a vertical profile of several meters. *Appl. Environ. Microbiol.* **72**: 2756-2764.

Wuchter, C., Abbas, B., Coolen, M.J.L., et al. (2006) Archaeal nitrification in the ocean. *Proceedings of the National Academy of Sciences* **103**: 12317-12322.

Zwart, G., and Bok, J. (2004) Protocol DGGE. In: Center for Limnology, Netherlands Institute of Ecology (NIOO-KNAW), pp. 1-6.